ELSEVIER

Coordination Chemistry Reviews
193–195 (1999) 1027–1068

COORDINATION CHEMISTRY REVIEWS

www.elsevier.com/locate/ccr

Polynuclear Ni^{II} and Mn^{II} azido bridging complexes. Structural trends and magnetic behavior

Joan Ribas [a,*], Albert Escuer [a], Montserrat Monfort [a], Ramon Vicente [a], Roberto Cortés [b], Luis Lezama [b], Teófilo Rojo [b]

[a] *Departament de Química Inorgànica, Universitat de Barcelona, Diagonal, 647, 08028-Barcelona, Spain*
[b] *Departamento de Química Inorgánica, Universidad del Pais Vasco, Apartado, 644, 48040-Bilbao, Spain*

Received 26 October 1998; received in revised form 8 December 1998; accepted 15 February 1999

Contents

* Corresponding author. Tel.: +34-93-4021264; fax: +34-93-4907725.
E-mail address: jribas@kripto.qui.ub.es (J. Ribas)

0010-8545/99/$ - see front matter © 1999 Elsevier Science S.A. All rights reserved.
PII: S0010-8545(99)00051-X

Abstract

The azide anion is a good bridging ligand for divalent metal ions, mainly Cu^{II}, Ni^{II} and Mn^{II}. It may give end-to-end (1,3) or end-on (1,1) coordination modes. As a general trend, the 1,1 mode exhibits ferromagnetic coupling while the 1,3 mode creates antiferromagnetic coupling. This review focuses on polynuclear Ni^{II} and Mn^{II} azido bridging complexes. Polynuclear structures known to have these two cations are: discrete (normally dinuclear), one-, two- and three-dimensional nets. The main characteristics of these structures are reported together with their magnetic behavior. From a large number of known structures, magneto-structural correlations are made. Taking into account that $M–N_3$ distances are always similar, the angles within the $M–(N_3)_n–M$ unit are the main determinant of the type and magnitude of the exchange coupling. Moreover, some one-, two- and three-dimensional complexes exhibit cooperative effects (long-range magnetic order), behaving as molecular magnets. This behavior is also analyzed. © 1999 Elsevier Science S.A. All rights reserved.

Keywords: Polynuclear Ni^{II} and Mn^{II} azido bridging complexes; Magnetic behavior; Molecular magnets

1. Introduction

A marked evolution has taken place recently in the field of molecular magnetism. Research has shifted focus from the synthesis and study of discrete polynuclear molecules in an attempt to improve our understanding of the mechanism involved in magnetic coupling [1,2] and the production of new paramagnetic clusters with high spin and strong anisotropy (*superparamagnetic molecules*) [3,4] to the synthesis and characterization of new low-dimensional materials (one- or two-dimensional) that may show ferromagnetic long-range cooperative phenomena (*molecular magnets*) [5–9].

Pseudohalide anions are excellent ligands for obtaining discrete, one-dimensional, two-dimensional or three-dimensional systems. Among these, the azido ligand is the most versatile in linking divalent metal ions. If we consider Ni^{II} and Mn^{II} ions, a large number of polynuclear M^{II} complexes with azido bridging ligands has been reported in the literature. These complexes can be divided according to their dimensionality: discrete molecules, one-dimensional, two-dimensional and three-dimensional systems. When the N_3^- anion acts as bridging ligand there are two typical coordination modes: end-to-end (EE or 1,3) and end-on (EO or 1,1).

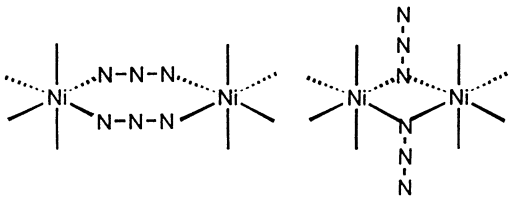

end-to-end *end-on*

Normally, the end-to-end (EE) coordination mode gives antiferromagnetic coupling while the end-on (EO) gives ferromagnetic coupling, but for very large M-$\mu_{1,3}$-N_3–M bond angles the magnetic coupling may be reversed. When the azido bridges are exclusively *end-to-end* or *end-on* it does not mean that all bridges are structurally and crystallographically identical. Within the same system (one or two-dimensional) two or more different structural bridges may be present, owing to different distances and/or angles found in the structure. These systems are antiferro- or ferromagnetic, but they belong to the so-called 'alternating magnetic systems', indicating the need to introduce two or more exchange coupling parameters (J) so as to fit the experimental results in contrast with the 'uniform magnetic systems' in which all azido bridges have the same coordination mode and the same structural parameters. Finally, for low-dimensional complexes, highly unusual systems containing simultaneously both kinds of coordination mode (EE and EO) have been reported. They are also of considerable interest in terms of their behavior as alternating ferro–antiferromagnetic (F–AF) coupled systems. Synthetically it is impossible to determine, with our present state of knowledge, which coordination mode will be adopted.

In this review we divide these systems according to their nuclearity and dimensionality. In each case we separate, where possible, the reported complexes on the basis of their magnetic behavior: antiferromagnetic, ferromagnetic or alternating systems.

Theoretically, just what constitutes the most suitable method for analyzing the superexchange interaction through an azido bridge has been much discussed in recent years. The first approach was undertaken by means of MO extended-Hückel calculations [10] and in 1986 Kahn and coworkers [11a] noted that the spin polarization model would describe the superexchange for the azido ligand more accurately, particularly for the EO coordination. More recently, spin density maps in the triplet ground state of $[Cu_2(t\text{-Bupy})_4(\mu\text{-}N_3)_2](ClO_4)_2$ (t-Buty = *p*-*tert*-butylpyridine) have been published [11b] and the authors state that 'the spin distribution in the triplet ground state in $[Cu_2(t\text{-Bupy})_4(\mu\text{-}N_3)_2](ClO_4)_2$ is dominated by a spin delocalization mechanism to which is superimposed a spin polarization effect within the π-orbitals of the azido group' and '…can the 1,1-azido group be considered as an almost universal ferromagnetic coupler, or is the stabilization of the parallel spin state only achieved in a limited range of bridging angle values?'. However, studies conducted on coupled dimers [12,13] for EE azido bridges seem to indicate that, at least for this coordination mode,

MO extended-Hückel calculations are appropriate. For this reason, we will use this model when correlating the magnetic properties. Recently, some ab initio calculations on these systems have been reported [11b,14]. Magneto-structural correlations have been developed by the authors [15–23] and elsewhere [14,24–26].

In order to compare all magnetic results reported in the literature it is necessary to establish just one Hamiltonian to calculate the exchange coupling parameter (J). In the literature, the two most frequently used are $H = -J_{ij}S_iS_j$ or $H = -2J_{ij}S_iS_j$. According to these Hamiltonians, the J value obtained when using the first Hamiltonian is twice than when using the second. However, in some papers J is given in K, though mainly in cm^{-1}. For these reasons, we decided to adopt the Hamiltonian $H = -J_{ij}S_iS_j$ (J in cm^{-1}) and to change the reported values in those cases where the $-2J$ Hamiltonian was used. The danger of adopting this assumption lies in those cases in which the authors do not clearly indicate which Hamiltonian they have used.

Here two dihedral angles are used for magnetostructural correlations: τ (the dihedral angle between the mean planes M–N1–N2–N3 and N1–N2–N3–M′) and δ (the dihedral angle between the plane defined for the six N azido atoms and the N1–M–N3′ plane). δ is normally used for complexes with double azido bridges and τ for complexes with single azido bridges.

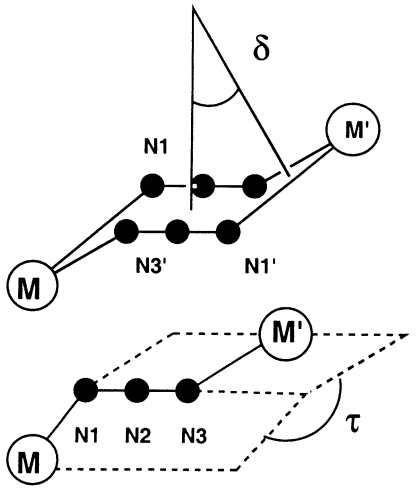

2. Dinuclear complexes

2.1. With 1,3-azido bridging ligands

Three models have been structurally characterized: with only one azido bridge; with two azido bridges and with three azido bridges.

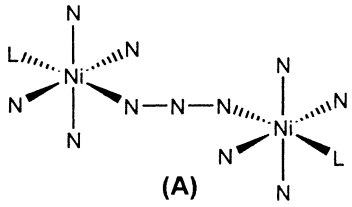

(A)

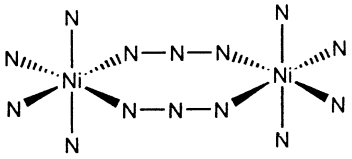

(B)

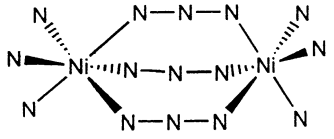

(C)

There are four fully characterized complexes with only one azido bridging ligand, $[Ni_2(N_3)_2(Me_4\text{-cyclam})_2(\mu\text{-}N_3)]I$ (Me_4-cyclam = 1,4,8,11-tetramethyl-1,4,8,11-tetraazacyclotetradecane) [26,27] in which two terminal azido ligands in *trans* position with regard to the bridge, complete the octahedral coordination of the Ni^{II} ions, $[Ni_2(trenpy)_2(\mu\text{-}N_3)](ClO_4)_3$ [28] (trenpy = *N*,*N*-bis(2-aminoethyl)-*N*′-2-(pyridylmethyl)ethane-1,2-diamine), $[Ni_2(L)(\mu\text{-}N_3)](N_3)(ClO_4)$ [29] and $[Ni_2(L)(H_2O)(\mu\text{-}N_3)](CF_3SO_3)_2$ (L = cryptate host) [29]. The main feature of the first two complexes, which is also present in the one-dimensional systems with only one azido bridging ligand in 1,3 coordination mode, is the non-linearity between the two Ni^{II} ions and

Table 1
Structural and magnetic parameters for dimers with the $[Ni(\mu_{1,3}\text{-}N_3)Ni]$ unit: Ni–N bond distances (Å), Ni–N–N and τ angles (°), J in cm^{-1}[a]

	Ni–N	Ni–N–N	τ	J	Reference
$[Ni_2(trenpy)_2(\mu\text{-}N_3)](ClO_4)_3$	2.133	131.6	180	−26.8	[28]
$[Ni_2(dmptacn)_2(\mu\text{-}N_3)](ClO_4)_3$	–	–	–	−42.5	[28]
$[Ni_2(Me_4cyclam)_2(N_3)_2(\mu\text{-}N_3)]I$	2.15	142	180	−17.0	[26]
$[Ni_2(L)(\mu\text{-}N_3)](N_3)(ClO_4)$	1.998	169.9	–	–	[29a]
	2.032	164.7	–	–	
$[Ni_2(L)(H_2O)(\mu\text{-}N_3)](CF_3SO_3)_2$	2.037	165.8	–	+11.8	[29b]
	1.998	157.6			

[a] Trenpy = *N*,*N*-bis(2-aminoethyl)-*N*′-2-(pyridylmethyl)ethane-1,2-diamine; dmptacn = 1,4-bis(2-pyridylmethyl)-1,4,7-triazacyclononane; Me_4-cyclam = 1,4,8,11-tetramethyl-1,4,8,11-tetraazacyclotetradecane; L = cryptate host)

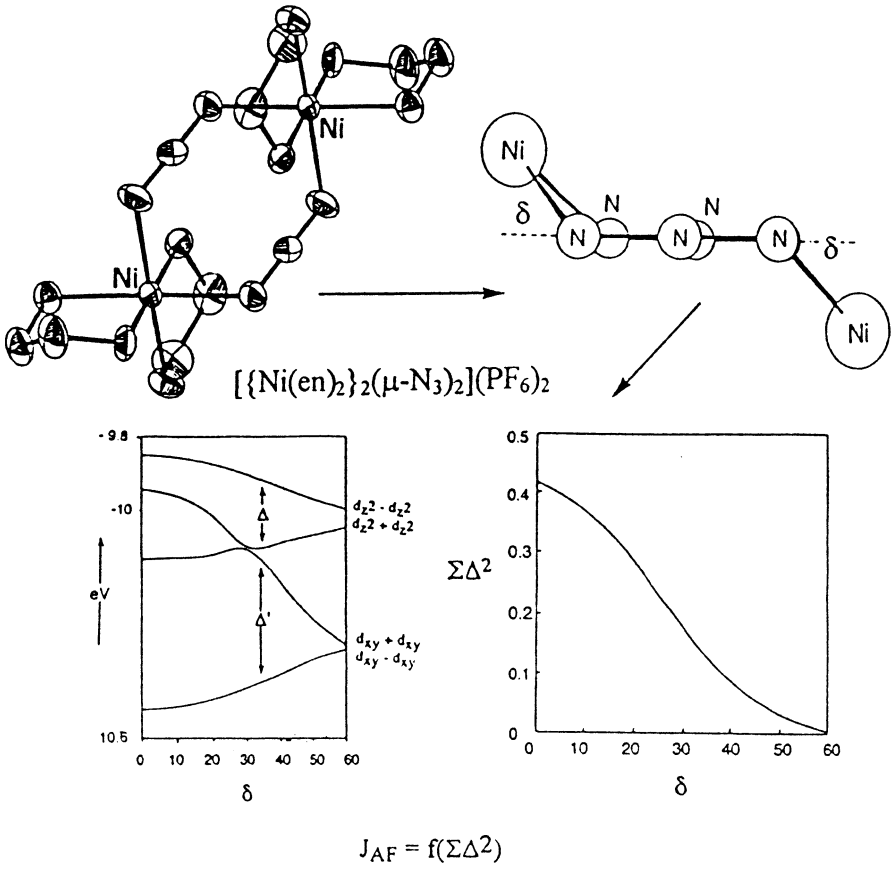

Fig. 1. ORTEP plot showing the structure of $[\{Ni(en)_2\}_2(\mu\text{-}N_3)_2](PF_6)_2$ (top); Walsh diagram for the four combinations of magnetic orbital upon variation of δ and variation of $\Sigma\Delta^2$ as a function of dihedral angle δ (bottom).

the azido bridge. In contrast, the 'cascade' complexes formed in the cryptate host, show the rather unusual quasi-linearity of the $Ni–N_3–Ni$ central unit (Ni–N–N angles close to 165°).

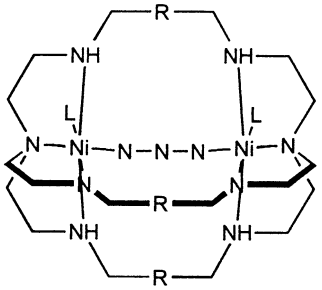

According to the authors [29a], this colinearity is due to the geometrical constraints imposed by the quite rigid dimetallic cryptate. It is also favored by $\pi-\pi$ interactions between azide and the three phenyl rings of the cryptate, the phenyl rings being nearly parallel and equidistant to all three aromatic planes. The main structural data and the exchange coupled parameter, J, are given in Table 1. It must be pointed out that the latest compound is the only example reported with ferromagnetic coupling through EE azido bridges as predicted. No magnetic results are reported for the complex $[Ni_2(L)(\mu\text{-}N_3)](N_3)(ClO_4)$ [29].

A single case with only one end-to-end azido bridging ligand and also a pyrazole bridge has been reported recently though no magnetic data are given [30].

The number of reported dinuclear complexes with two azido bridging ligands has increased greatly over the past 10 years. The formula of the core is $[Ni_2(\mu\text{-}N_3)_2]^{2+}$. In all the reported complexes but one, the two azido ligands are coplanar. The exception is $[Ni_2(L')_2(N_3)_2(\mu\text{-}N_3)_2]$ ($L' = 1,4,7$-trimethyl-1,4,7-triazacyclononane) [24] in which the two azido bridging ligands cross each other. To complete the coordination of the Ni^{II} ions there are generally bi-, tri- or tetradentate amine ligands. In some cases there are some azido terminal ligands. The counter-anion is, usually, a non-ligating anion such as ClO_4^-, PF_6^- or $[B(C_6H_5)_4]^-$. A representative

Table 2
Structural and magnetic parameters for dimers with $[Ni(\mu_{1,3}\text{-}N_3)_2Ni]$ unit: Ni–N bond distances (Å); Ni–N–N and δ angles (°), J in cm^{-1}[a]

	Ni–N	Ni–N–N	δ	J	Reference
$[Ni_2(en)_4(\mu\text{-}N_3)_2](PF_6)_2$	2.181	121.1	45.0	−4.6	[21]
	2.183	119.3			
$[Ni_2(1,3\text{-tn})_4(\mu\text{-}N_3)_2](BPh_4)_2$	2.167	127.7	3.0	−114.5	[21]
	2.144	139.0			
$[Ni_2(L)_2(N_3)_2(\mu\text{-}N_3)_2]$	2.167	124.4	6.8	−90.0	[33]
	2.135	138.4			
$[Ni_2(L')_2(N_3)_2(\mu\text{-}N_3)_2]$	2.111	124.5	[b]	−36.4	[24]
	2.118	128.2			
$[Ni_2(tren)_2(\mu\text{-}N_3)_2](BPh_4)_2$	2.069	123.3	20.7	−35	[26]
	2.195	135.7			
$[Ni_2(222\text{-tet})_2(\mu\text{-}N_3)_2](BPh_4)_2$	2.103	128.5	22.4	−83.6	[39]
	2.155	129.9			
$[Ni_2(aep)_4(\mu\text{-}N_3)_2](PF_6)_2$	2.180	126.7	34.6	−29.1	[75]
	2.128	123.8			
$[Ni_2(D,L\text{-cth})_2(\mu\text{-}N_3)_2](ClO_4)_2$	2.141	141.6	3.3	−113.0	[76]
	2.098	127.4			
$[Ni_2(D,L\text{-cth})_2(\mu\text{-}N_3)_2](PF_6)_2$	2.128	124.3	11.5	−75.1	[76]
	2.143	142.2			

[a] (L = 1,5,9-triazacyclododecane; L′ = 1,4,7-trimethyl-1,4,7-triazacyclononane; tren = 2,2′,2″-triaminotriethylamine; 222-tet = triethylenetetramine; aep = aminoethylpyridine; cth = 5,5,7,12,12,14-hexamethyltetraazacyclotetradecane).

[b] This is the only case in which the doubly bridged moiety $(N_3)_2$ is not planar. The dihedral angles, as defined by the authors, are 15.6 and 21.4°. This $(N_3)_2$ planarity is characteristic of all other dinuclear complexes.

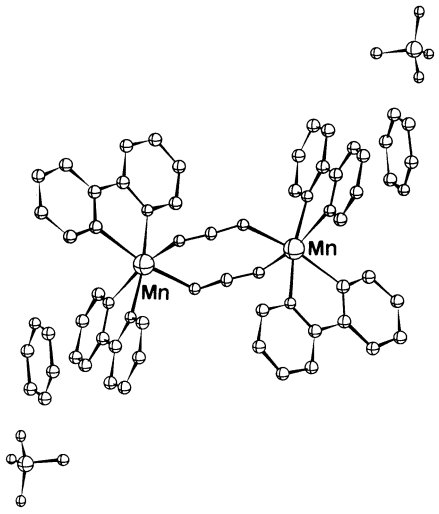

Fig. 2. ORTEP plot showing the structure of $[Mn_2(bpy)_4(\mu\text{-}N_3)_2](ClO_4)_2 \cdot bpy$.

example of these complexes is shown in Fig. 1. The main structural data and the exchange coupled parameter, J, are given in Table 2.

Based on these data a new magneto–structural relationship has been developed between the exchange coupling parameter, J (in cm^{-1}), and the structural data [21]. The main factor determining the J value is the [Ni–(μ-N_3)$_2$–Ni] dihedral angle δ. The results of extended Hückel molecular orbital calculations are shown in Fig. 1 as $\Sigma\Delta^2$ versus δ, where Δ represents each of the gaps created between the symmetric and antisymmetric combinations of the Ni^{II} magnetic orbitals ($z^2 \pm z^2$ and $x^2-y^2 \pm x^2-y^2$). According to the magnetochemical theories [31], J_{AF} is proportional to this gap ($J_{AF} \propto \Sigma\Delta^2$). Experimental data agree with this model. Thus, the more planar the structure (dihedral angle δ close to 0°), the more antiferromagnetic is the coupling. When this dihedral angle increases, the J value decreases [21]. In all cases we assume that the two N_3 ligands are coplanar.

To our knowledge, only one case of Mn^{II} dinuclear complex showing EE azido bridges has been reported: $[Mn_2(bpy)_4(\mu\text{-}N_3)_2](ClO_4)_2 \cdot bpy$ [32] (Fig. 2). The crystal structure shows the Mn^{II} ions double bridged by two azido ligands in their EE bridging mode, where the bridging angles Mn–N–N and N–N–Mn are 128.6 and 131.3°, respectively. The $[Mn-(N_3)_2-Mn]^{2+}$ unit shows a chair configuration. The existence of a non-coordinated bipyridine ligand, which is sited parallel to the bpy ligands of the dimer, is a peculiarity of this structure. Preliminary magnetic results for this dinuclear compound confirm AF interactions.

In the literature, only one dinuclear complex with a triple 1,3-N_3 bridging ligand is reported, $[Ni_2(1,4,7,\text{-trimethyl-}1,4,7\text{-triazacyclononane})_2(\mu\text{-}N_3)_3](ClO_4)$ [24,33]. The Ni–N–N angles lie between 115.6 and 119.2° (average value = 118.1°). The J value is -67.9 cm^{-1}.

2.2. With 1,1-azido bridging ligands

All these complexes, as indicated above, show ferromagnetic coupling. Two kind of systems have been structurally characterized and reported: with two azido bridges and with three azido bridges (only two complexes).

The number of Ni^{II} dinuclear complexes reported with two EO azido bridging ligands has increased considerably over the past 10 years. The formula of the core is $[Ni_2(\mu_{1,1}\text{-}N_3)_2]^{2+}$. All the reported complexes, but two (see Table 3), show a [Ni–$(N_3)_2$–Ni] planar unit with an inversion center. To complete the coordination of the Ni^{II} ions there are generally bi-, tri- or tetradentate amine ligands. In some cases there are some azido terminal ligands. The counter-anion is, usually, a non-ligating anion such as ClO_4^- or PF_6^-. A representative structural example of these complexes is shown in Fig. 3. The main structural data and the exchange coupled parameter, *J*, are given in Table 3.

Table 3
Structural and magnetic parameters for dimers with $[Ni(\mu_{1,1}\text{-}N_3)_2Ni]$ unit: Ni–N bond distances (Å) and Ni–N–Ni angles (°), *J* in cm^{-1}[a]

	Ni–N	Ni–N–Ni	Ni–(N_3)–Ni inv. centre	*J*	Refer-enece
$[Ni_2(en)_4(\mu\text{-}N_3)_2](ClO_4)_2$	2.144 2.123	104.3	Yes	43.7	[49]
$[Ni_2(terpy)_2(N_3)_2(\mu\text{-}N_3)_2]\cdot 2H_2O$	2.198 2.038	101.3	Yes	40.2	[15a,b]
$[Ni_2(terpy)_2(N_3)(H_2O)(\mu\text{-}N_3)_2]ClO_4$	2.069 2.172 2.114 2.060	103	No	27.2	[15c]
$[Ni_2(pepci)_2(N_3)_2(\mu\text{-}N_3)_2]\cdot 2H_2O$	2.107 2.163 2.109 2.128	102.20 101.0	No	72.6	[77]
$[Ni_2(Me_3[12]N_3)_2(\mu\text{-}N_3)_2](ClO_4)_2$	2.092 2.067	103.8	Yes	43.9	[78]
$[Ni_2(232\text{-}N_4)_2(\mu\text{-}N_3)_2](ClO_4)_2$	2.166	104.9	Yes	33.8	[78]
$[Ni_2(Me\ dpt)_2(N_3)_2(\mu\text{-}N_3)_2]$	2.207 2.197	104.0	Yes	46.7	[35] [79]
$[Ni_2(232\text{-}tet)_2(\mu\text{-}N_3)_2](PF_6)_2$	2.177 2.183	104.6	Yes	34.3	[80]
$[Cu_{1.5}Ni_{0.5}(terpy)_2(N_3)_2(\mu\text{-}N_3)_2]\cdot 2H_2O$	2.83 1.97	95.1	Yes	40.2	[81]

[a] (pepci = N′-(2-pyridin-2-ylethyl)pyridine-2-carbalimide; $Me_3[12]N_3$ = 2,4,4-trimethyl-1,5,9-triazacyclododec-1-ene; 232-N_4 = N,N′-bis(2-aminoethyl)-1,3-propanediamine; Medpt = methyl-bis(3-aminopropyl)amine).

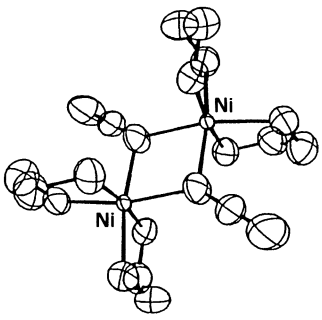

Fig. 3. Representative structural example of the $[Ni_2(\mu_{1,1}\text{-}N_3)_2]^{2+}$ core.

All these dinuclear complexes have a Ni–N–Ni angle close to 101–104° and are coupled ferromagnetically. J values lie between 20 and 40 cm^{-1} approximately. In the ferromagnetic systems, owing to the zero field splitting (ZFS) manifest at low temperatures, the magnitude of J should be treated with care. Almost all the authors who have investigated this kind of complex use the Ginsberg formula [34] which introduces the J, D, g and $z'J'$ (coupling between dimers) parameters. With these four parameters the correlation between them could be significant.

Due to the inversion center in the planar [Ni–$(N_3)_2$–Ni] core, this part of the structure is like a rhombus. The compound $[Ni_2(Medpt)_2(N_3)_2(\mu\text{-}N_3)_2]$ undergoes an asymmetrization process as the temperature falls. This can be visualized in the magnetic measurements.

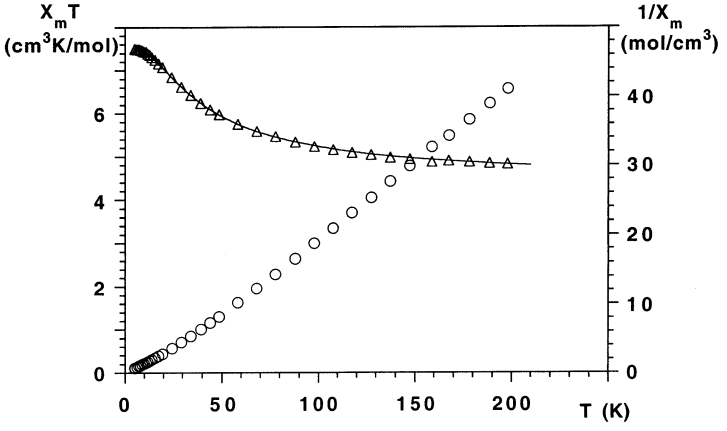

Fig. 4. $\chi_M T$ (△) and $1/\chi_M$ (○) of $[Mn_2(terpy)_2(N_3)_2(\mu\text{-}N_3)_2]\cdot 2H_2O$ as a function of the temperature. The full curve represents the theoretical curve for $J = 2.43$ cm^{-1} and $g = 2.0$.

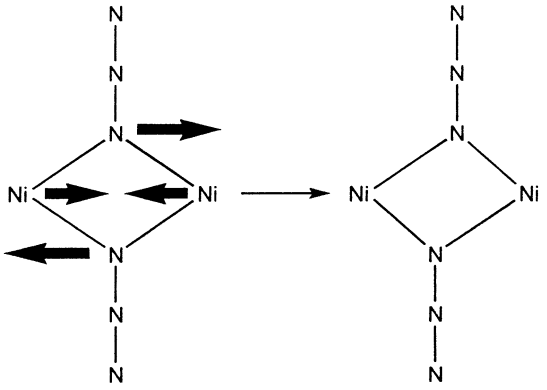

This phase transition creates an hysteresis cycle in the molar susceptibility measurements. This hysteresis seems to indicate that the magnetic transition is not reversible, at least during the measurement time. Calorimetric data obtained from some of these complexes also indicate a non-reversible transition. This asymmetrization transition has been explained in terms of a second-order Jahn–Teller distortion, taking into account the local symmetry of the dinuclear [Ni–$(N_3)_2$–Ni] entity (D_{2h}, rhombic symmetry) before the arrangement [35].

In the case of the Mn^{II} ion, the same dinuclear core has been obtained for two complexes: $Na[Mn(pzate)(N_3)_2(H_2O)]_2 \cdot H_2O$ (Hpzate = pyrazine-2-carboxilic acid) [36], which has the bond angle Mn–N–Mn of 100.2(1)° (magnetic data were not reported), and $[Mn_2(terpy)_2(N_3)_2(\mu\text{-}N_3)_2]2H_2O$ [37] in which the Mn^{II} ions are doubly bridged by EO–N_3 ligands, with the tridentate terpy ligand occupying three of the four equatorial sites of the coordination polyhedron of each metal and a terminal azido group to complete the hexacoordination. The value of the bridging angle is 104.6°. The magnetic results for this Mn^{II} compound are illustrated in Fig. 4. As can be observed, the $\chi_M T$ value increases upon cooling, reaching a maximum and remaining stable at lower temperatures. This clearly corroborates intradimer ferromagnetic interaction through EO–azido bridges. The magnetic susceptibility data were analyzed in terms of the dipolar coupling approach for a Mn^{II} dimer, the best fit result gave a set of parameters $J = 2.43$ cm^{-1} and $g = 2.0$.

Finally, only two complexes with three azido bridging ligands have so far reported: $[Ni_2L_2(\mu\text{-}N_3)_3]ClO_4$ (L = 1,4,7-trimethyl-1,4,7-triazacyclononane) [24] and $[Ni_2L_2(\mu\text{-}N_3)_3]ClO_4$ (L = (*N*,*N*′-dimethyl-1,4,7-triazacyclononane)calix[4]arene [38]. The geometry of the triple bridge is similar in both complexes, with an average Ni–N–Ni angle of 85.9 and 86.2°, respectively. The Ni···Ni distances are, evidently, shorter than for dinuclear complexes with only two azido bridging ligands (2.896 and 2.852 Å, respectively). Both complexes show ferromagnetic coupling ($J = 30.7$ and 17.2 cm^{-1}, respectively).

3. Trinuclear complexes

Only two complexes of this kind have been reported in the literature: $[Ni_3$(2,2,2-

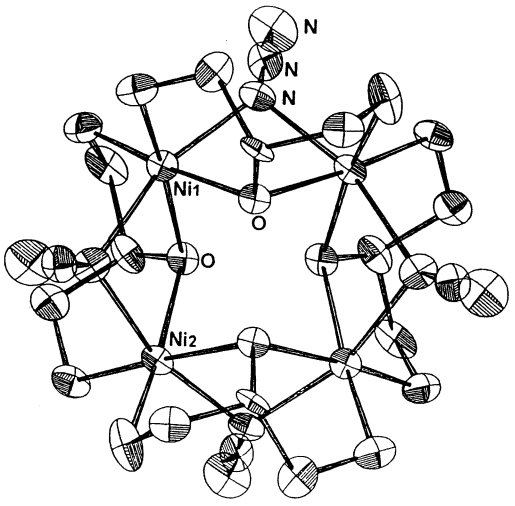

Fig. 5. ORTEP plot showing the structure of the tetranuclear compound $[Ni_4$(2-oxo-1,3-diaminopropane)$_2$(2-hidroxo-1,3-diaminopropane)$_2(\mu_{1,1}$-$N_3)_4](ClO_4)_2$.

tet)$_3(\mu$-$N_3)_3](PF_6)_3$ and the perchlorate analogue [39]. The crystal structure of these two complexes is not known but EXAFS and XANES spectra reveal the occurrence of azido-bridged trinuclear nickel(II) compounds with Ni···Ni separations of 5.16 and 5.12 Å, respectively. Each Ni^{II} ion is placed in an octahedral NiN_6 environment: four nitrogen atoms of the amine and two nitrogen atoms of the two azido bridges. The proposed structure is, thus, an irregular triangle for both complexes. In order to fit the magnetic results it was necessary to introduce two J values: $J_{1,2} = -72$ and -60.3 cm^{-1} and $J_3 = -36$ and -29 cm^{-1}, respectively, in agreement with the assumed 1,3 coordination mode for the azido bridging ligand.

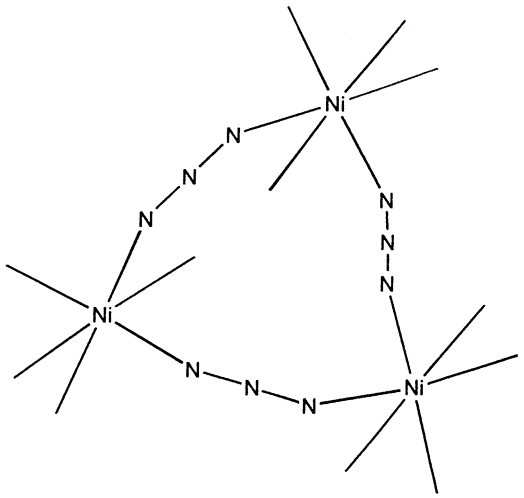

4. Tetranuclear complexes

Three Ni^{II} tetranuclear complexes with EO–azido bridging ligand have been reported. The first has the formula $[Ni_4(2\text{-oxo-}1,3\text{-diaminopropane})_2(2\text{-hydroxo-}1,3\text{-diaminopropane})_2\ (\mu_{1,1}\text{-}N_3)_4](ClO_4)_2$ [40] (Fig. 5). The four Ni^{II} atoms are in a distorted octahedral environment and are related by an S_4 symmetry axis forming a quasi-perfect square. The oxygen atom of the amine ligand (OHpn and Opn) also acts as a bridging ligand between two Ni^{II} ions. Magnetic measurements indicate ferromagnetic coupling with $J = 21.3\ cm^{-1}$. Magnetization measurements are indicative of an $S = 4$ spin ground state. The second complex reported to date has a cubane-like structure. Its formulation is $[Ni_4(dbm)_4(EtOH)_4(\eta^1,\mu_3\text{-}N_3)_4]$ (dbm = dibenzoylmethane) [41,42].

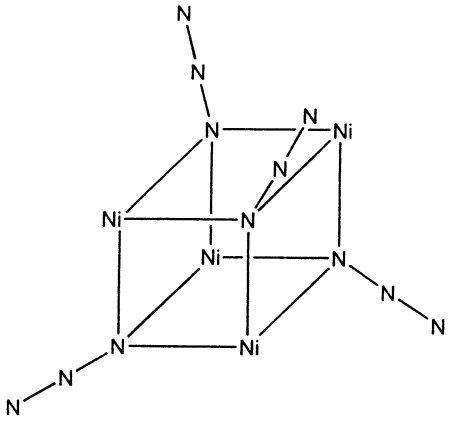

Each azido ligand is bound symmetrically to three Ni^{II} ions in an end-on fashion. Magnetic behavior was well reproduced by the one-J model, giving $J = 11.9\ cm^{-1}$. The third case corresponds to a compound with formula $[Ni_4(dpkO)_4(\mu\text{-}N_3)_4]$ (dpk = di-2-piridylketone) [43]. It consists of tetranuclear units where the Ni^{II} ions are bridged by both μ-oxo and μ-end-on azido ligands, to give a face-share dicubane-like coordination core with two missing vertices (Fig. 6). Preliminary magnetic measurements for this complex indicate a predominance of ferromagnetic interactions (Fig. 6). The observation of ferromagnetic interactions within these complexes is consistent with both the previously proposed accidental orthogonality and spin polarization theories. In the first and third cases, the presence of oxo (hydroxo) bridges, allowing two different pathways for the magnetic coupling, prevents any possible magneto–structural correlations.

For the manganese ion only one tetranuclear compound has been reported [44], with formula, $[Mn_2(HL)(N_3)_2]_2{\cdot}3MeCN$ (H_2L = 1,7,14,20-tetramethyl-2,6,15,19-tetra-aza[7,7](2,6)pyridiniphane-4,7-diol). It consists of two dinuclear entities with two oxo and one EO azido bridges, linked by means of a single EO azide bridge (Fig. 7). The Mn–N–Mn bond angle between dimeric units shows the anomalously

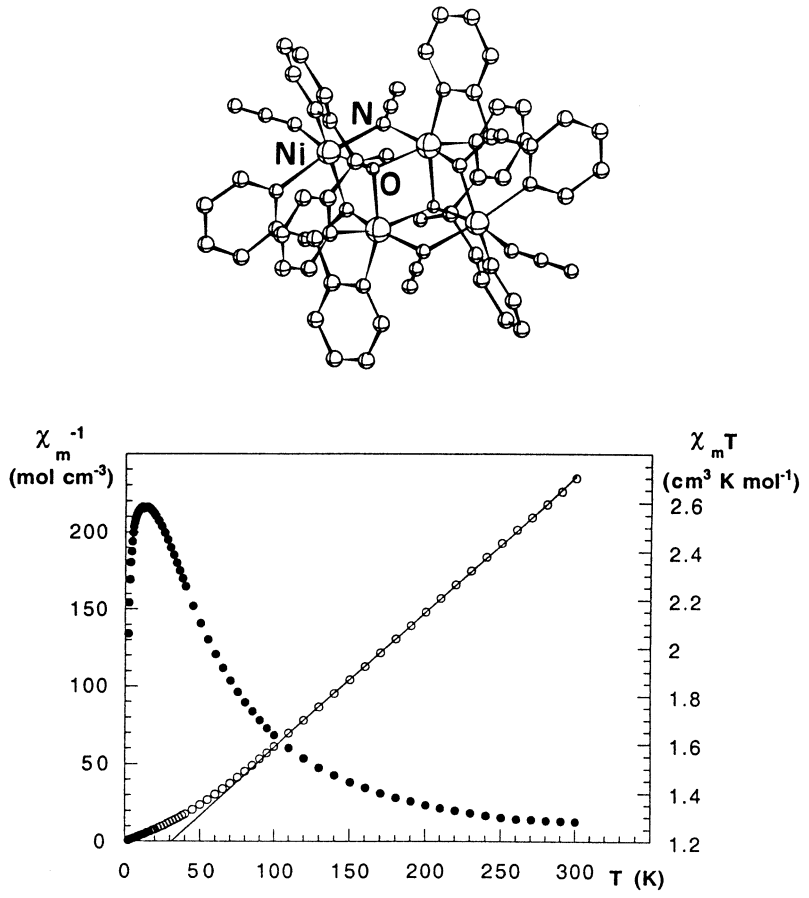

Fig. 6. ORTEP plot (top) showing the structure of $[Ni_4(dpkO)_4(\mu\text{-}N_3)_4]$ and $\chi_M T$ ((●) and χ_M (○) for this compound as a function of the temperature (bottom).

high values of 126.3(2) and 128.3(2)°, whereas the intradimer Mn–N–Mn bond angle has values of 84.7(2) and 83.1(2)°. The global magnetic behavior measured between 300–6 K shows antiferromagnetic coupling but detailed J values for each bridge type were not reported.

5. One-dimensional uniform systems

Uniform 1D systems are understood to be those systems in which all ions have the same magnetic pathway, i.e. only one type of azido bridging ligand and only one set of structural parameters. In order to fit the magnetic data only one exchange coupling parameter (J) is necessary.

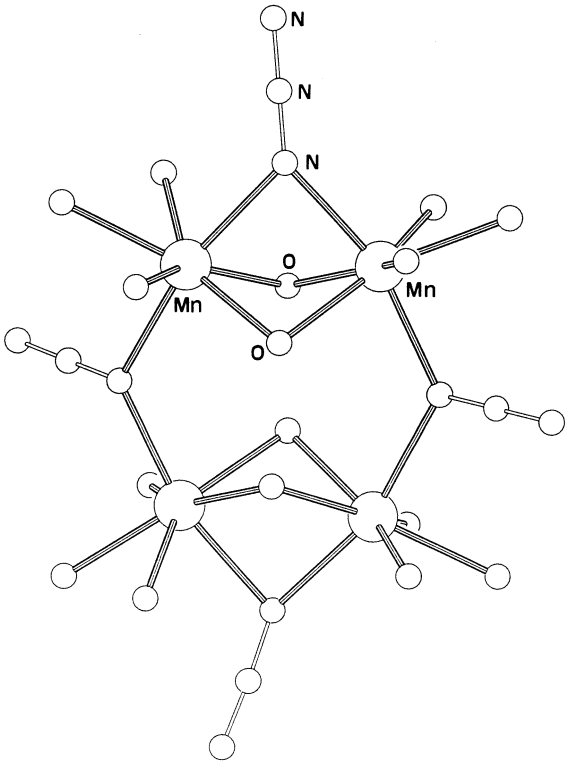

Fig. 7. Molecular structure of $[Mn_2(HL)(N_3)_2]_2$ (H_2L = 1,7,14,20-tetramethyl-2,6,15,19-tetraaza-[7,7](2,6)pyridiniphane-4,7-diol).

5.1. With 1,3-azido bridging ligands (AF)

Although very similar, we can distinguish two types of 1D system: *trans* or *cis*, according to the position of the two adjacent azido bridging ligands. To date, for the Ni^{II} ion,

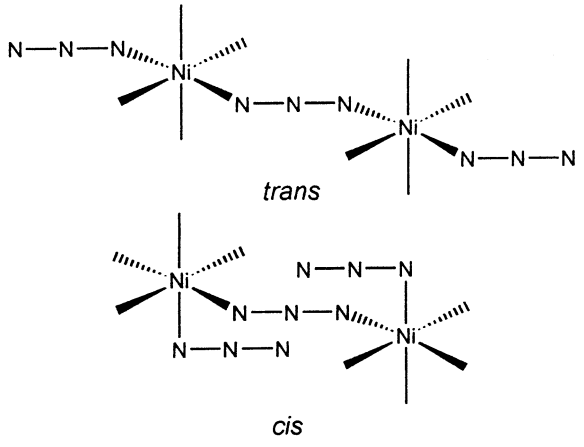

only 1D systems with one 1,3-azido bridging ligand have been reported. To complete the hexacoordination of each Ni^{II} ion, two bidentate or one tetradentate nitrogen ligands have been used. The main structural data and the magnetic behavior (exchange coupled parameter, J) are given in Table 4 for *trans*-complexes and in Table 5 for *cis*-complexes. A representative structural example of *trans* and *cis* chains are shown in Fig. 8, respectively.

Magneto–structural correlations have been made in both kinds of complex, *trans* and *cis*, with similar results [16,45]. For these correlations extended Hückel calculations were performed by means of the CACAO program [46] on a dimeric fragment modeled as indicated in the drawing.

Table 4
Structural and magnetic parameters for 1-D *trans*-Ni-($\mu-N_3$)-Ni systems: Ni–N–N and dihedral angles (°); J in cm^{-1}[a]

	Ni–N–N	τ	J	Reference
$[Ni(tmd)_2(\mu\text{-}N_3)]_n(ClO_4)_n$	120.9	180	−100	[82]
$[Ni(tmd)_2(\mu\text{-}N_3)]_n(PF_6)_n$	126.1	180	−55.8[b] (−70.6)	[83]
$[Ni(2,2'\text{-mettn})_2(\mu\text{-}N_3)]_n(ClO_4)_n$	137.2	180	−49.4	[84]
$[Ni(2,2'\text{-mettn})_2(\mu\text{-}N_3)]_n(PF_6)_n$	136.5	180	−19.4[b] (−41.1)	[83]
$[Ni(cyclam)_2(\mu\text{-}N_3)]_n(ClO_4)_n$	140.7 128.2	166.9	−39.2	[85]
$[Ni(232\text{-tet})_2(\mu\text{-}N_3)]_n(ClO_4)_n$	134.6 124.1	142.4	−26.9	[17]
$[Ni(323\text{-tet})_2(\mu\text{-}N_3)]_n(ClO_4)_n$	135.8 119.8	169.3	−62.7	[17]
$[Ni(macro)_2(\mu\text{-}N_3)]_n(ClO_4)_n$	115.6 116.8	175.7	−97.8	[86]
$[Ni(cth)_2(\mu\text{-}N_3)]_n(ClO_4)_n$[c]	A) 128.5 130.7 B) 131.4	150.5 146.2	−41.1 −36.4	[87]

[a] (2,2′-mettn = 2,2′-dimethyl-1,3-diaminepropane; 232-tet = *N*,*N*′-bis(2-aminoethyl)-1,3-propanediamine; 3,2,3-tet = *N*,*N*′-bis(amonipropyl)1,3-ethanediamine; macro = 2,3-dimethyl-1,4,8,11-tetraazacyclotetradeca-1,3-diene; cth = *meso*-5,7,7,12,14,14-hexamethyl-1,4,8,11-tetraazacyclotetradecane).

[b] In these two complexes there is a phase transition when the temperature decreases, which changes the structural parameters and the magnetic results. The results at high temperature, (before the transition) are shown in parentheses while the results at low temperature (after the transition) are shown without parentheses.

[c] This complex shows two structurally distinct 1-D uniform chains in the crystal net in a 2:1 ratio. These chains are indicated as A and B.

Table 5
Structural and magnetic parameters for 1-D *cis*-Ni-($\mu-N_3$)-Ni systems: Ni–N–Ni and dihedral angles (°); J in cm^{-1}[a]

	Ni–N–N		τ	J	Reference
$[Ni(333\text{-tet})_2(\mu\text{-}N_3)]_n(PF_6)_n$	151.8		142.8	−18.5	[45]
	151.3				
$[Ni(2\text{-methyl})_2(\mu\text{-}N_3)]_n(ClO_4)_n$	131.8		125.9	−16.8	[88]
	125.9				
$[Ni(2\text{-methyl})_2(\mu\text{-}N_3)]_n(PF_6)_n$	135.0		146.8	−3.2	[88]
	122.6				
$[Ni(bipy)_2(\mu\text{-}N_3)]_n(ClO_4)_n$[b]	123.7	120.1	133.9	−33.0	[16]
	126.6	121.3	138.9		
$[Ni(bipy)_2(\mu\text{-}N_3)]_n(PF_6)_n$[b]	122.6	122.6	134.9	−22.4	[16]
	120.6	127.4	138.0		
$[Ni(aep)_2(\mu\text{-}N_3)]_n(ClO_4)_n$	127.8		122.4	< −1	[75]
	126.2				

[a] (333-tet = *N*,*N*'-bis(3-aminopropyl)-1,3-propanediamine; 2-methyl = 1,2-diamino-2-methyl-propane; aep = 2-(aminoethyl-pyridine)).

[b] These two chains actually belong to the alternating AF chains because, according to the authors, the asymmetric unit is formed by two Ni-N_3-Ni entities that are attached consecutively in a chain. The fit of the magnetic data was made assuming only one value of J, as a uniform chain, because the variation of Ni-N-N and dihedral angles is small.

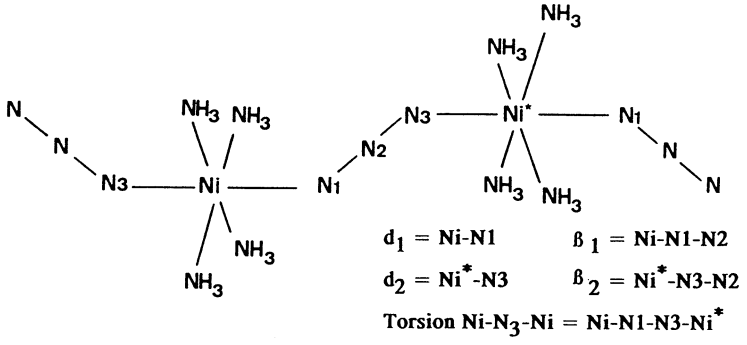

Since bond distances are similar in all the complexes reported, the wide range of bond angles (Ni–N–N and dihedral Ni–N_3–Ni torsion) must play a significant role in the superexchange interaction between the nickel atoms.

In a *trans* chain in which the $d(z^2)$ orbitals are oriented in the chain direction, only the z direction is operative as an exchange pathway, and J_{AF} is solely a function of $\Delta^2(z^2) = [E\Phi(z^2)_{(s)} - E\Phi(z^2)_{(a)}]^2)$.

Fig. 9 represents the MO calculations made when varying the Ni–N–N angle between 90 and 180° and assuming that the Ni–N_3–Ni (torsion angle) is 180°. For this figure the maximum coupling is expected for Ni–N–N angles of 108° while for greater values the antiferromagnetic interaction must decrease. An accidentally orthogonal valley, centered at 164° is found. This plot agrees with the generally accepted assumption that the main interactions occurs through the π pathway using

the non-bonding MO of the azido ligand and the σ pathway is poorly operative. The effect of the dihedral Ni–NNN–Ni angle has also been parametrized between 180 and 130°. For all Ni–N–N angles the maximum coupling can be expected for a torsion value of 180°, decreasing gradually thereafter as the torsion angle increases. The magnitude of this effect is lower than the effect of the bond angle and might be considered as a secondary factor refining the main factor. As an example, 30° of variation in Ni–N–N angle between 120 and 150° reduces the Δ^2 value by ca. 90%, whereas, for both angles, 30° of variation in the Ni–N_3–Ni torsion angle reduces the Δ^2 value by ca. 35%.

On the other hand, calculations involving three nickel atoms and placing the azido bridges in *trans* or *cis* arrangement [16,45] show the same general behavior for $\Sigma\Delta^2$ (in a *cis* conformation $\Delta^2(xy)$ is not zero), indicating, as expected, that the main factor in the magnitude of the AF interaction are the bond parameters of each bridge and not how this unit is repeated along one axis. The maximum J values correspond at approximately the same Ni–N–N angle for *trans* or *cis* geometry (108 and 110°, respectively).

In the *cis* complexes, the torsion angle is greater than that in *trans* complexes (Tables 4 and 5) creating, thus, lower AF coupling. Taking into account the helical topology of these *cis* systems, there is further factor that needs to be considered, the compactness of this helix. This is due to the sum of all the small differences in angles and distances that are, however, difficult to visualize independently: the more compact the helicoidal structure, the greater the antiferromagnetic coupling.

Finally, these uniform one-dimensional systems obtained from Ni^{II} ($S = 1$) have been studied extensively by the physicist as they provide good experimental examples

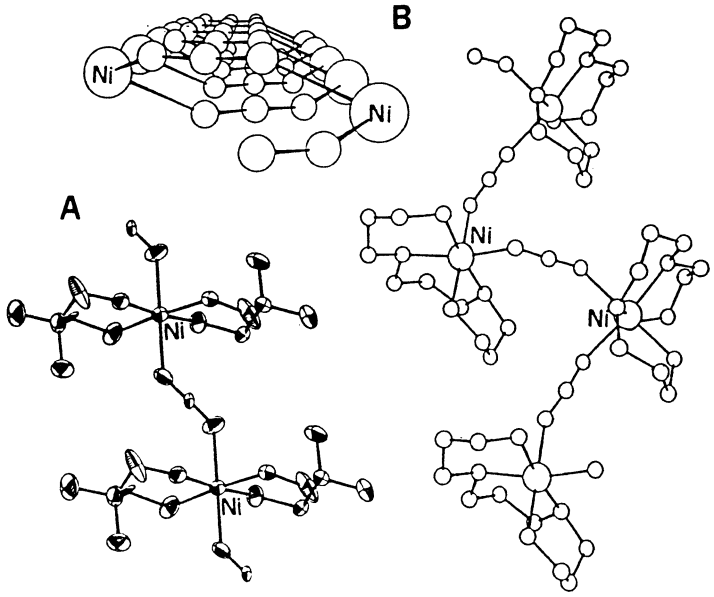

Fig. 8. Representative structural example of a *trans* uniform chain, A and a *cis* uniform chain, B.

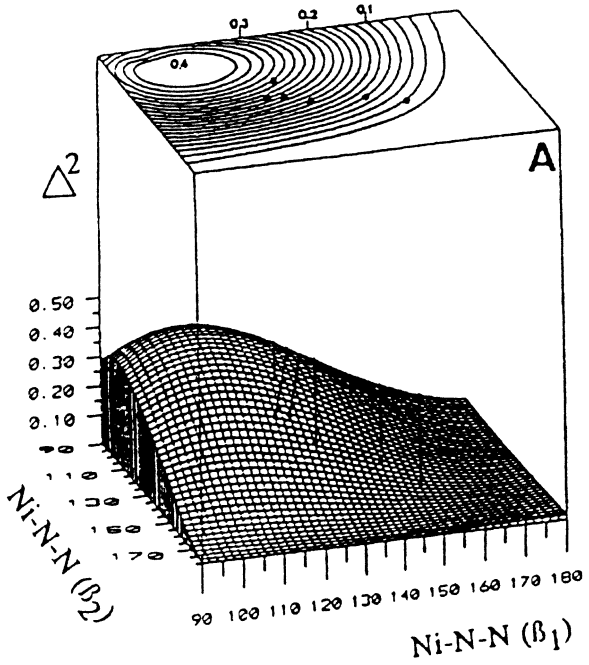

Fig. 9. Plot of Δ^2 in function of β_1 and β_2 for a [NiNi] monobridged EE azido system.

for investigating the so-called Haldane's gap (a quantic gap created between the ground state ($S = 0$) and the first excited state, when the S value is integer [47]).

In contrast with nickel, only one homogeneous chain with a double EE azide bridge has been reported for the manganese ion [48]. This has the formula $[Mn(pyOH)_2(N_3)_2]_n$ (pyOH = 2-hydroxypyridine). In this case the pyOH ligand coordinates the manganese atom in monodentate form through the oxygen atom, giving a *trans*-system (Fig. 10). The main bond parameters related with the superexchange pathway are Mn–N 2.245(2)–2.250(2) Å, bond angles: Mn–N–N

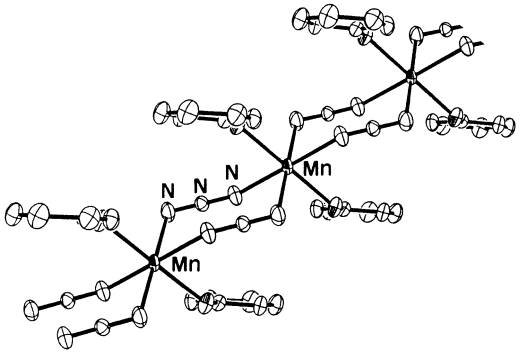

Fig. 10. ORTEP plot showing the structure of the double EE azido bridging 1D compound $[Mn(pyOH)(N_3)_2]_n$ (pyOH = 2-hydroxypyridine).

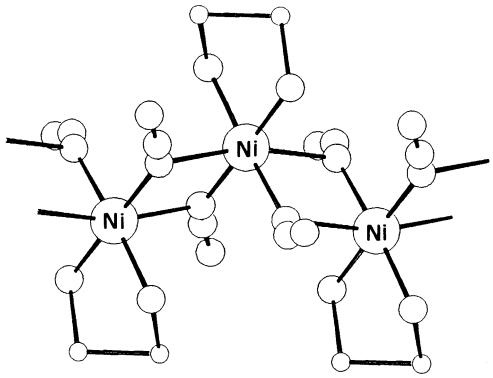

Fig. 11. Schematic representation of the double 1,1-azido bridging 1D compounds.

122.3(1)–123.8(1)°, δ parameter = 38.0°. The coupling was moderately antiferromagnetic with $J = -7.0\ cm^{-1}$. The factors thought to influence the superexchange were studied in a similar fashion as to that with nickel, and the results were also found to be similar: the maximum AF coupling occurs for planar Mn–$(N_3)_2$–Mn rings, (δ parameter = 0), while coupling decreases as the δ parameter increases.

5.2. With 1,1-azido bridging ligands (F)

For the Ni^{II} ion, only two complexes of this type have been reported fully [49]. The general formula is $[Ni(L)(\mu\text{-}N_3)_2]_n$ (L = ethylenediamine, 1,3-diaminopropane and 2,2′-dimethyl-1,3-diaminopropane). Fig. 11 is a schematic representation of these chains.

In Table 6 the main structural and magnetic parameters are reported. Unfortunately, the crystals for the two structures presented poor crystallinity preventing a good refinement. Thus, the crystal data (Table 6) must be treated with care. The three complexes are ferromagnetic, as expected given the coordination mode of the

Table 6
Structural and magnetic parameters for 1-D Ni-($\mu_{1,1}$-N_3)–Ni systems[a]

	Ni–N–Ni		J[b]	$\lvert D\rvert$	Reference
	Unit A	Unit B			
$[Ni(en)(N_3)_2]_n$	103.1	100.9	35.6	6.3	[49]
	95.2	100.9	23.8	0	
$[Ni(tn)(N_3)_2]_n$	108.1	100.1	35.2	4.4	[49]
	105.0	101.4	39.8	0	
$[Ni(2,2'\text{-mettn})(N_3)_2]_n$	–		29.4	6.7	[49]
			33.8	0	

[a] Ni–N–Ni angles (°); J in cm^{-1}. (en = ethylenediamine; tn = 1,3-diaminopropane; 2,2′-mettn = 2,2′-dimethyl-1,3-diaminopropane).

[b] The first J value is found by assuming $|D| \neq 0$; the second one by assuming $|D| = 0$.

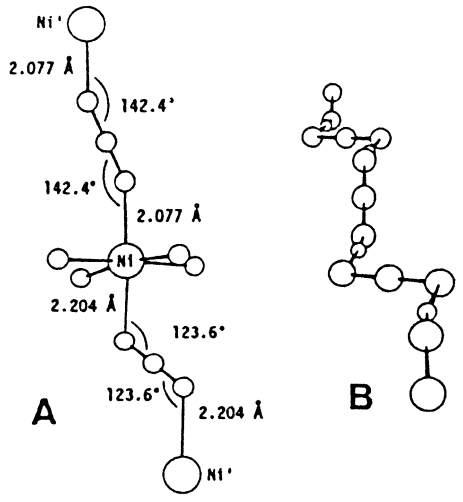

Fig. 12. Schematic representation of the *trans* uniform chain $[Ni(333\text{-tet})(\mu\text{-}N_3)]ClO_4$ (333-tet = *N*,*N*′-bis(3-aminopropyl)-1,3-propanediamine) (A) showing the different set of structural parameters (B) showing the torsion angle between neighboring azido groups.

azido bridging ligand. Preliminary results with high fields (1.0–1.5 T) indicate a very strong dependence of the external field in the low temperature region. Such behavior may be indicative of metamagnetic systems. For this reason the susceptibility curves were drawn and fitted at very low fields. The magnetic parameters were obtained assuming $D = 0$ or including the D parameter in the de Neef formula [50], which allows this kind of uniform chains to be fitted for $S = 1$. For this reason there are two J values in Table 6.

With the same metal–azide squeleton the manganese derivative $[Mn(2\text{-bzpy})(N_3)_2]_n$ chain has been characterized in which 2-bzpy is 2-benzoylpyridine [51]. The bridges are not equivalent but show little deviation from the mean Mn–N–Mn value of 100°. Due to the large volume of the 2-bzpy ligand the chains are well isolated with an interchain Mn···Mn distance of 9.93 Å, which minimizes the interchain coupling. As expected, the intrachain coupling was found to be ferromagnetic, showing a χT value of 32.8 emu K mol^{-1} at 2 K.

6. One-dimensional alternating systems

6.1. With only 1,3-N_3 bridges

Two types of this complex have been reported to date: (a) *With two different geometries in adjacent 1,3-N_3 azido bridges*. This is the case of $[Ni(333\text{-tet})(\mu\text{-}N_3)]ClO_4$ (333-tet = *N*,*N*′-bis(3-aminopropyl)-1,3-propanediamine) [45]. This one-dimensional system can be schematized as $-Ni-N_a-N_b-N_a-Ni-N_c-N_d-N_c-Ni-N_a-N_b-N_a-Ni-$. Thus, the most interesting feature of this compound is the existence of inversion centers at the central nitrogen of two consecutive yet different azido groups. The two $Ni-N_a$ and $Ni-N_c$ bond distances are quite distinct, 2.077

and 2.204 Å, respectively. The two bond angles, Ni–N_a–N_b and Ni–N_c–N_d, are 142.4 and 123.6°, respectively, the larger angle corresponding to the shorter bond distance. This feature is shown in Fig. 12. Each fragment of the five Ni–N_3–Ni atoms is coplanar, and consequently the torsion angle is 180°. The torsion angle between neighboring azido groups is 93.4°, as shown in Fig.12 B. An equation for the analysis of magnetic susceptibility data of alternating chains with local $S=1$ has been proposed by Borras et al. [52] for calculations on a cyclic system of four spin pairs that gives a good approximation up to $kT/J_1=0.4$. By using this expression, the value of the coupling parameters has been optimized up to the values $J=-80.7$ cm^{-1}, $J'=-37.4$ cm^{-1} (alternating parameter $J'/J=\alpha=0.46$) and $g=2.4$. It is interesting to point out that when using the equation for a uniform chain, the J value obtained is very close to the mean of the calculated values for an alternating system ($J=-62.1$ cm^{-1}). According to the magneto-structural correlations given in the previous section for uniform chains, two very different values of J are expected for the two different bridges of this alternating chain because the Ni–N–N angles are very different (142 and 123°, respectively). The greater experimental J value ($J=-80.7$ cm^{-1}) can be assigned to the bridge of 123° (closer to 108–110° for which the maximum susceptibility is expected) and the smaller value ($J=-37.4$ cm^{-1}) to the greater angle (142.4°). The alternating parameter α is 0.46 and the theoretical ratio between the calculated gaps when using the extended-Hückel OM model is 0.52, showing excellent agreement with the experimental value [45]. This compound has been extensively studied as a model of the gapless point of the Affleck–Haldane conjecture [53].

In the case of manganese, one singular compound with alternating double EE azido bridge has also been reported: the $[Mn(3\text{-Etpy})_2(N_3)_2]_n$ compound (3-Etpy = 3-ethylpyridine) [48], which shows *trans* coordination and two different sets of bond parameters in each alternating Mn–$(N_3)_2$–Mn unit with a different degree of chair distortion with δ parameters of 6.9 and 11.6° (Fig. 13). In good agreement with the above model, the coupling was found to be antiferromagnetic and closely related to the δ parameter, with $J=-13.8/-11.7$ cm^{-1}, respectively. (b) *With consecutive single and double 1,3-azido bridging ligands*. This is the case of $[(Ni_2(dpt)_2(\mu\text{-}N_3)(\mu\text{-}N_3)_2)]_n(ClO_4)_n$ (dpt = bis(3-aminopropyl)amine) [23] (Fig. 14). The structure consists of a 1-D –Ni–$(N_3)_2$–Ni–N_3–Ni– system. The part with a single azido bridge is like all systems described for uniform chains: the Ni–N–N angle is 119.2° and the torsion angle Ni–N_3–Ni is 0°(180°). The most interesting feature of this structure is the relative position of the two azido bridges in the Ni–$(N_3)_2$–Ni fragment. The structure of the Ni–$(N_3)_2$–Ni fragment derives from the symmetric rotation of the coordination polyhedra of the nickel atoms around the x-axis, as shown in Fig. 15 B. As a result of this movement, the nickel atoms and the central nitrogen atoms of the azido groups are always maintained in the xy plane, whereas the N(azido) atoms linked to the nickel atoms leave the original plane (distortion type ρ), ρ being in this case the angle defined for the N*–N axis and the xy plane. For this complex, the corresponding mean ρ angle is roughly 20°. Extended-Hückel MO calculations have been performed on a dinuclear fragment modeled as in Fig. 15 B. The calculations were made by varying the ρ angle, maintaining all other

parameters as constants. The corresponding $\Sigma\Delta^2$ plot versus ρ is given in Fig. 15 C together with the variation for the δ distortion (Fig. 15 A), in order to compare both kinds of distortion. $\Sigma\Delta^2$ has a maximum for $\rho = 0$ as expected, reaching a value of 0 when $\rho = 32°$, and subsequently increases slowly. This behavior is different from that found for the δ distortion, for which $\Sigma\Delta^2$ decreases continuously in the interval 0–60°. The J values found by using the Borras equation [52] are: $J = -84.6\ cm^{-1}$ and $J' = -41.4\ cm^{-1}$ ($\alpha = 0.49$). According to our previous

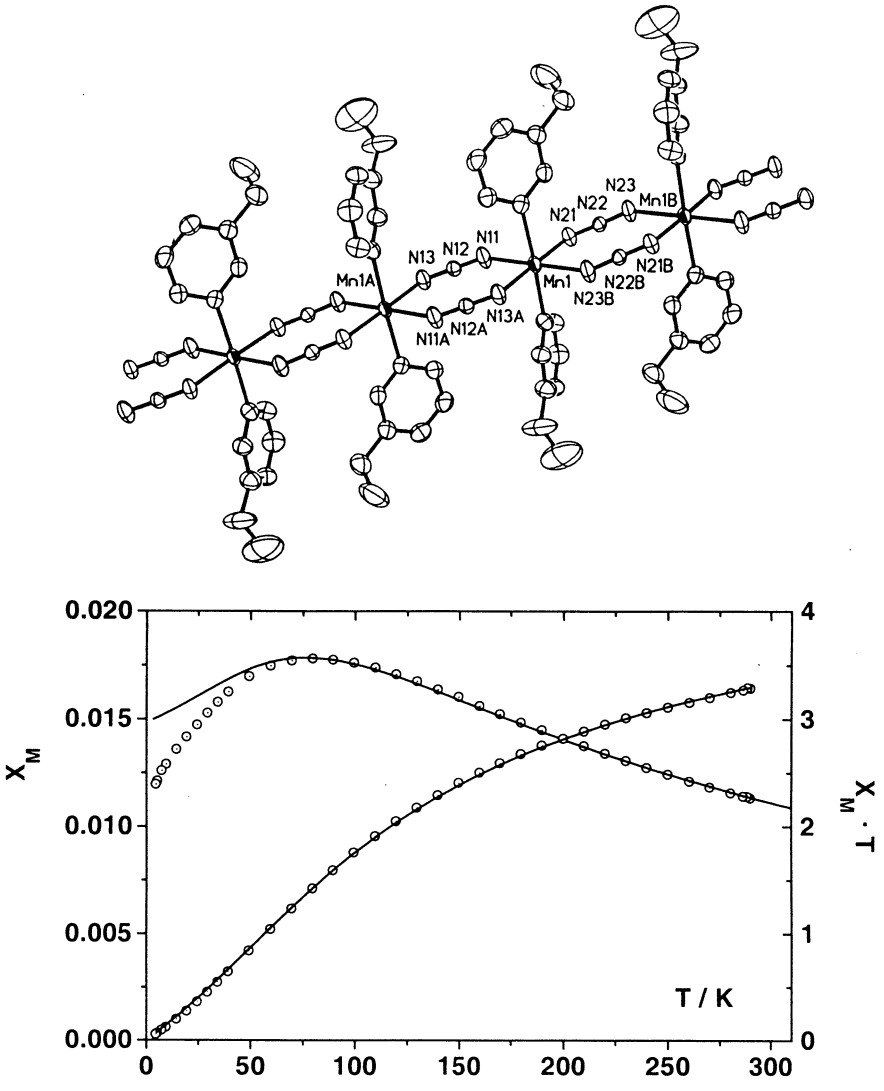

Fig. 13. ORTEP plot (top) showing the structure of the compound $[Mn(3\text{-Etpy})(N_3)_2]_n$ (3-Etpy = 3-ethylpyridine) and $\chi_M T$ (○) and χ_M (○) of this compound as a function of the temperature (bottom).

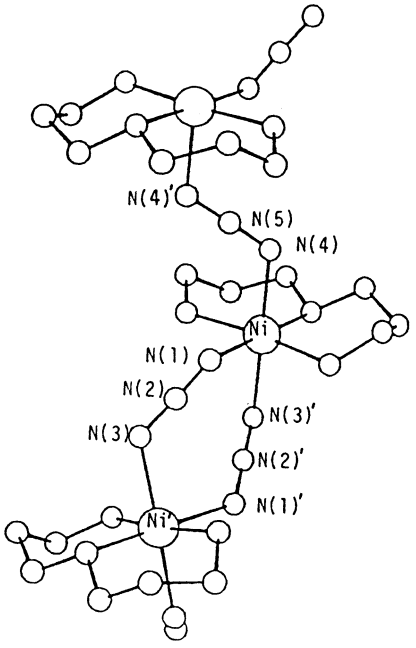

Fig. 14. Structure of the 1D system with consecutive single and double 1,3-azido bridging ligands $[Ni_2(dpt)_2(\mu\text{-}N_3)(\mu\text{-}N_3)_2]_n(ClO_4)_n$.

discussion, these two J values can be assigned unequivocally to the single and double azido bridges, respectively. The Ni–N–N angle of 119.2° (single bridge) is one of the lowest reported to date, thus the J value must be one of the greatest ($-84.6\ cm^{-1}$).

6.2. With 1,3-N_3 and 1,1-N_3 bridges

When in the synthetic procedure the Ni/diamine/azide ratio is 1/1/2 not only were new ferromagnetic chains obtained but, depending on the diamine used in the synthesis, new ferro–antiferromagnetic species were also synthesized. The alternation can be very simple, F–AF (Fig. 16 A), or much more complicated like, for example, F–F–F–AF (Fig. 16 B). In all these cases, the magnetic data have been interpreted and fitted by numerical extrapolation of $S = 1$ rings of finite length [54]. For these calculations an isotropic Heisenberg system with quantic spin $S = 1$ has been assumed. The main structural and magnetic parameters for this kind of one-dimensional alternating chain are shown in Table 7. From this Table it is possible to realize that the AF coupling parameter J agrees with the previous results described above: the higher the δ angle the lower the J value. The J values for the F part also agree with those reported for dinuclear complexes. In all cases the angle is close to 100°.

The same kind of system has also been obtained for Mn^{II} ion in the complex $[Mn(bpy)(\mu_{1,1}\text{-}N_3)(\mu_{1,3}\text{-}N_3)]_n$ [55] (Fig. 17). The azido ligands are arranged *cis* and

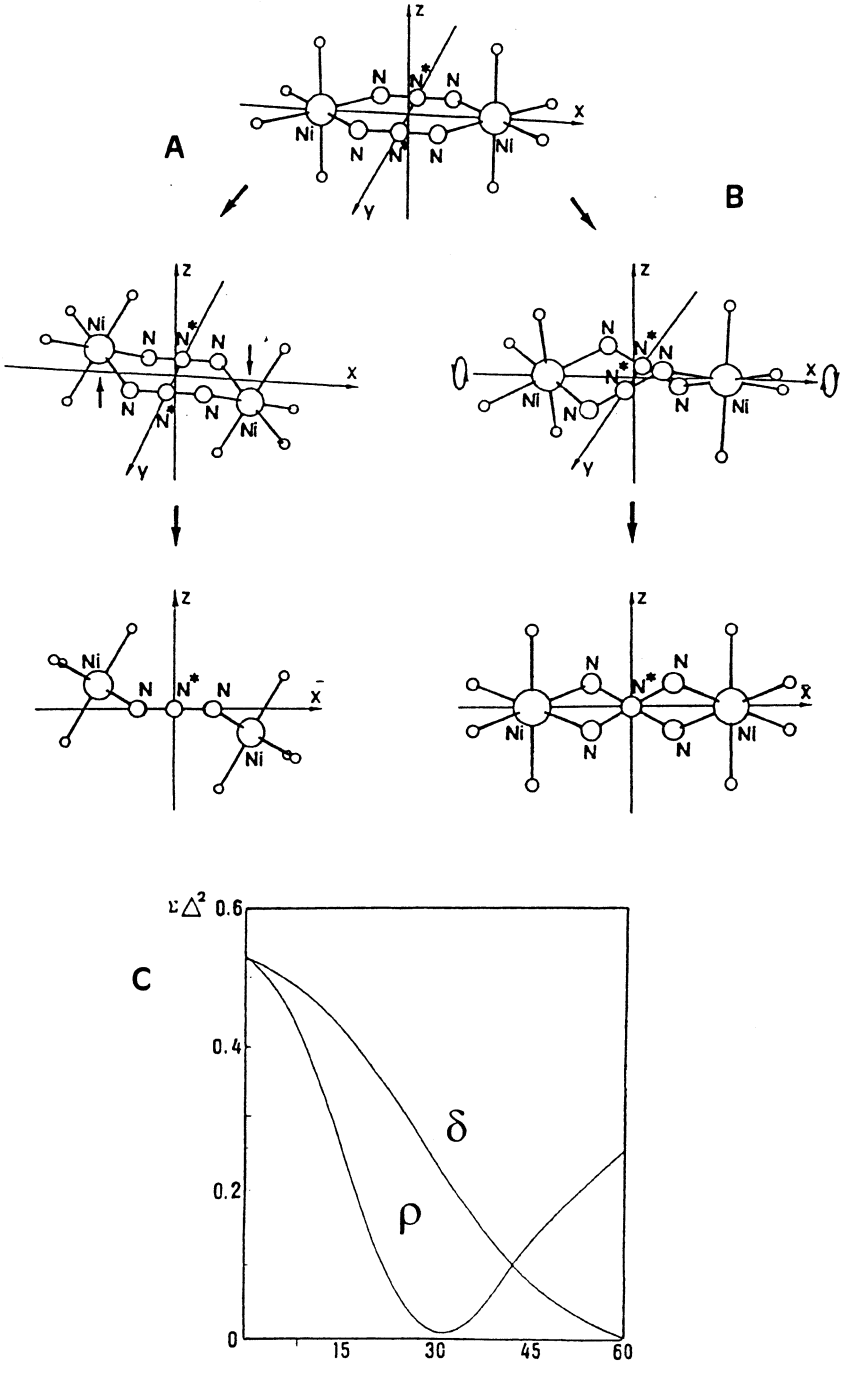

Fig. 15. Schematic representation for the two types of distortion found for the planar $[Ni_2(\mu_{1,3}\text{-}N_3)_2]^{2+}$ core (A, δ-type; B, ρ-type); plot of $\Sigma\Delta^2$ versus ρ or δ for a $[Ni_2(\mu_{1,3}\text{-}N_3)_2]^{2+}$ core (C).

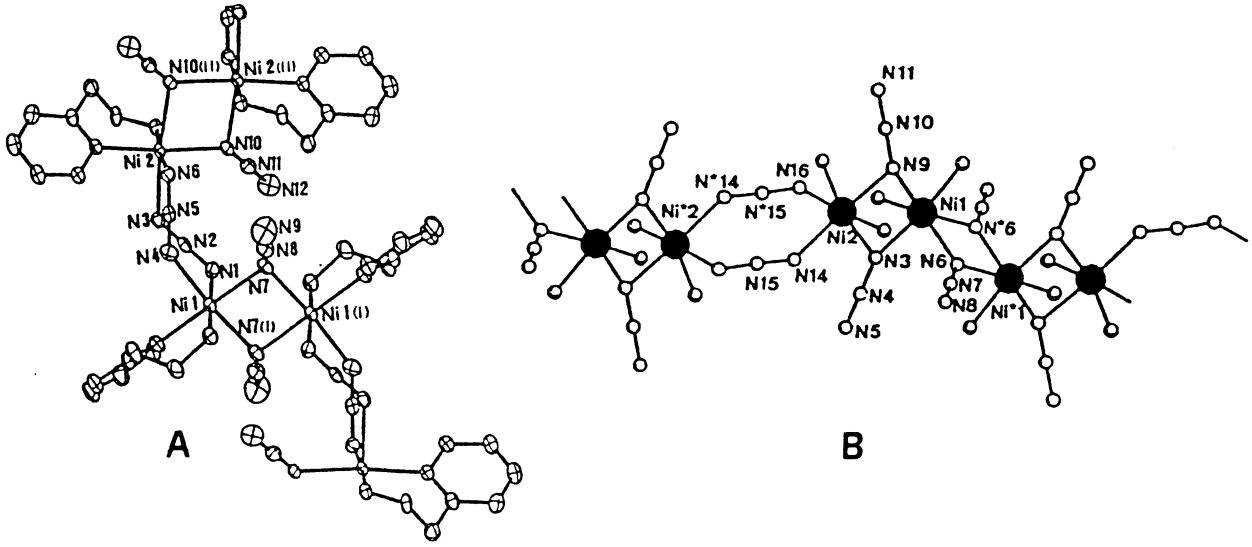

Fig. 16. Structure of 1D systems with consecutive F and AF azido bridging ligands (A) and with the F–F–F–AF azido bridging set (B).

are perpendicular to each other. The Mn–N–Mn′ angle in the EO bridge is 101.0°. For the EE bridges the Mn–N–N angles are 131.1(5) and 127.3(5)° for a chair conformation of the Mn–$(N_3)_2$–Mn unit and a torsion angle of 41.9°. Due to these structural features, alternating ferromagnetic (through EO bridges) and antiferromagnetic interactions (through EE bridges) should be expected. The thermal variation of both χ_M and $\chi_M T$ values, shown in Fig. 17, can only be explained assuming two alternating exchange constants: a positive J_1 for EO and a negative J_2 for EE pathways. However, no formula was available in the literature for an $S = 5/2$ ferro–antiferromagnetic alternating chain and for this reason a model was developed [55b]. The best agreement obtained by least squares refinement corresponds to the following set of parameters: $J_1 = 9.58\ cm^{-1}$; $J_2 = -11.80\ cm^{-1}$, $g = 2.01$. A new topology –double EO and single EE alternated– has recently been reported for $[Ni_2(Medien)(\mu_{1,1}\text{-}N_3)_2(\mu_{1,3}\text{-}N_3)]_n(ClO_4)_n$ [56] (Fig. 18). The structural parameters are unchanged for the two coordination modes and, as can be expected, the magnetic behavior corresponds to a F–AF alternating system. The data have been fitted with an expression built on the basis of the increasing ring systems calculations [65]. The main structural and magnetic parameters are shown in Table 7.

Finally, a unique case with one end-to-end and three end-on bridges in alternation has been reported. It is the complex $[Ni_2(tmeda)_2(\mu_{1,1}\text{-}N_3)_3(\mu_{1,3}\text{-}N_3)]_n$ (tmeda = *N*,*N*,*N*′,*N*′-tetramethylethylenediamine) [57] (Fig. 19). The most important features occur in the Ni–N–Ni angles.

The average value in the EO bridge is 84.2°, which is one of the lowest values for any metal ion with azido bridging ligand in EO mode. In the EE bridge the Ni–N–N

Table 7
Structural and magnetic parameters for F–AF 1-D systems[a]

	Type	Ni–N-N	Ni–N–Ni	δ	τ	J, J',J''	Reference
$[Ni(bipy)(\mu\text{-}N_3)_2]_n$	F–AF	118.2	101.5	35.2	180	26	[89]
		129.9				–2.6	
$[Ni(NN\text{-}dmen)(\mu\text{-}N_3)_2]_n$	F–AF	121.1	98.2	≈0	180	17	[90]
		139.4				−156	[54b]
$[Ni(aep)(\mu\text{-}N_3)_2]_n$	F–AF	125.6	98.7	[b]	[b]	5	[90]
		124.4				−28	[54b]
		121.6					
		117.9					
$[Ni(Medien)(\mu\text{-}N_3)]ClO_4$	F–AF	138.1	100.8	–	162.8	−34.7	[56]
		125.7	98.9			38.2	
$[Ni(NN'\text{-}dmen)(\mu\text{-}N_3)_2]_n$	F–F–F–AF	130.9	100.5	8.4	180	−120	[54a]
		132.9	101.2			20	
			102.9			37	

[a] Ni–N–Ni, Ni–N_3–Ni δ and τ angles (°), J in cm^{-1}. (*N*,*N*-dmen = *N*,*N*-dimethylethylenediamine; aep = 2-aminoethylpyridine, *N*,*N*′-dmen = *N*,*N*′-dimethylethylenediamine; Medien = Methyldiethylenetriamine).

[b] This Ni–$(N_3)_2$–Ni is fully asymmetric. Four nitrogen (azido) atoms and one Ni form a plane while the other two nitrogen (azido) atoms and the other Ni are clearly separated from this plane. The distances to the mean plane are 1.32 Å (Ni) and 1.62 Å (N-azido).

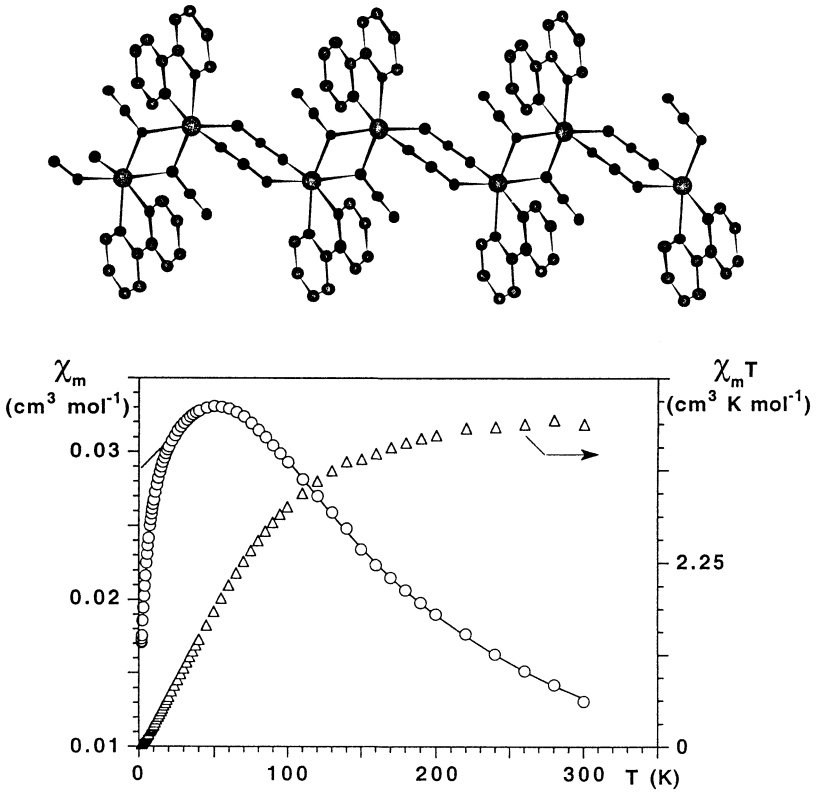

Fig. 17. Structure of $[Mn(bpy)(\mu_{1,1}\text{-}N_3)(\mu_{1,3}\text{-}N_3)_2]_n$ (top) and $\chi_M T$ (△) and χ_M (○) for this compound as a function of the temperature (bottom).

angle is 138° with a Ni–N_3–Ni dihedral angle of 180°. The data have been fitted with the Borrás formula [52] for an antiferromagnetic alternating $S = 1$ chain and with the standard formula for a dinuclear Ni^{II} unit (i.e. assuming that J_{EO} value, is zero). The parameters of the best fit and their reliability factors (R) are $J_1 = -31.8$ cm^{-1}, $J_2 = -6.9$ cm^{-1}, $g = 2.35$ and $R = 1.5 \times 10^{-4}$ for the alternating chain and $J = -29.3$ cm^{-1}, $g = 2.26$ and $R = 6.6 \times 10^{-3}$ for a dinuclear unit. The following

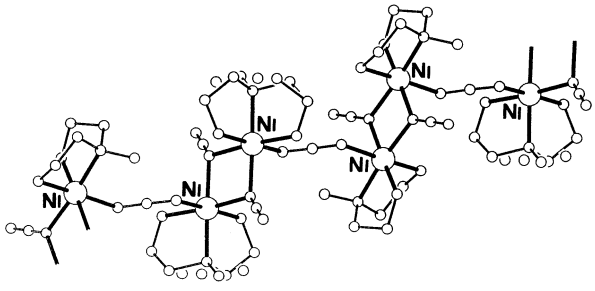

Fig. 18. Structure of the compound $[Ni_2(Medien)(\mu_{1,1}\text{-}N_3)_2(\mu_{1,3}\text{-}N_3)]_n(ClO_4)_n$.

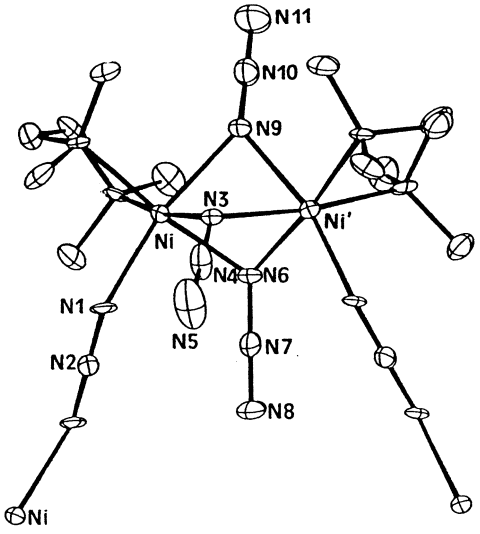

Fig. 19. OPTEP plot showing the structure of the triply EO and single EE azide bridging 1D compound $[Ni(tmeda)(\mu\text{-}N_3)_2]_n$.

values were determined for the maximum susceptibility: 0.01141 (experimental), 0.01160 (alternating chain), and 0.01192 $cm^3\ mol^{-1}$ (dinuclear unit). In both cases the experimental value in this zone is lower than the theoretical, and the difference is even greater for the dinuclear model. This suggests AF coupling is present in both parts of the chain (J_1 and J_2 negative).

6.3. Other alternating chains

An example of a different (and more evident) strategy to obtain alternating chains is the complex $[(Ni_2(dpt)_2(\mu\text{-ox})(\mu\text{-}N_3))_n](PF_6)_n$ in which two different bridging units alternate: oxalato and azido, respectively [20] (Fig. 20). The perchlorate analogue is also reported but without crystal structure. The oxalato group is coordinated in bis-bidentate form as occurs habitually, and the azido ligand is coordinated in end-to-end mode. Two kind of non-equivalent nickel atoms are present

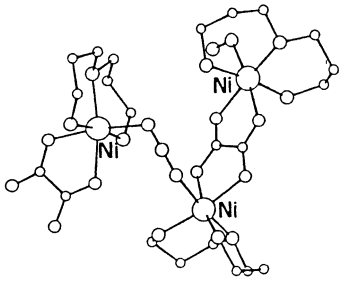

Fig. 20. Structure of the alternating chain in which two different bridging units (oxalato and azido) alternate: $[Ni_2(dpt)_2(\mu\text{-ox})(\mu\text{-}N_3)]_n(PF_6)_n$.

in the chain, which show different bond parameters and different coordination modes of the amminate ligand. The most remarkable features of the azido bridge are the asymmetric end-to-end coordination, with Ni–N–N = 120.1 and 119.41°, respectively, and the unusually high value (102.1°) for the torsion angle of Ni–N_3–Ni entity. Applying the Borrás equation [52] for an alternating 1-D chain with $S = 1$ the J values obtained for the hexafluorophosphate complex are: $J_1 = -27.4$ cm^{-1}, $J_2 = -2.7$ cm^{-1}, $g = 2.19$ ($\alpha = 0.1$) (those for the perchlorate analogue are very similar). Taking as reference the bibliographic J values for Ni–ox–Ni and Ni–N_3–Ni systems reported to date, assignation of the coupling parameters is immediate: for all the nickel–oxalato dinuclear systems, the J parameters have been found in the range -30 to -39 cm^{-1}. This practically constant J value is a consequence of the low flexibility of the oxalato ligand, roughly planar in all cases, which shows no significant differences in the bond parameters in the bridging region. The low value for J_2 is due, undoubtedly, to the very high torsion angle of the Ni–N_3–Ni entity (102.1°).

7. Two-dimensional systems

While the discrete molecules or 1-D systems with azido bridge have been found, so far, to be mainly nickel derivatives, the high dimensional compounds are clearly dominated by the manganese(II) compounds. In addition to their structure, the magnetic properties of this kind of compound are especially interesting at low temperatures. Indeed it is not rare to find ordered systems with the properties of weak molecular magnets.

7.1. With only azido as bridging ligand

7.1.1. With single EE bridges

For Ni^{II} the simplest case reported in the literature is the salt $Cs_2[Ni(N_3)_4]\cdot H_2O$ [58]. The anionic part consists in a 2-D structure formed by $Ni(N_3)_6$ octahedra connected via four azido groups placed in a distorted plane. No magnetic data have been reported.

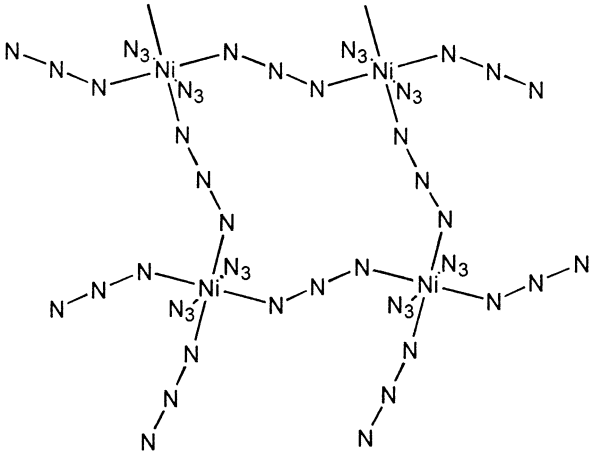

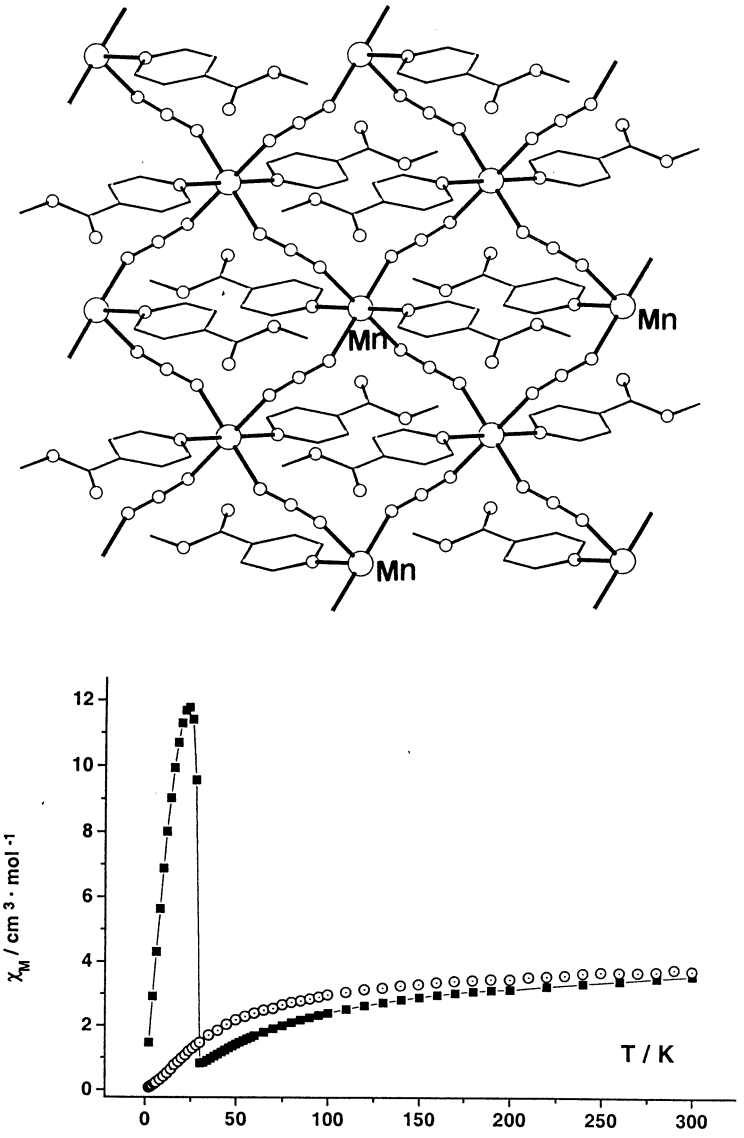

Fig. 21. Structure of the two-dimensional compound $[Mn(4\text{-acpy})_2(N_3)_2]_n$ (4-acpy = 4-acethylpyridine) and χ_M of this compound as a function of the temperature and field.

For the manganese ion two compounds with the general formula $[Mn(R\text{-}py)_2(N_3)_2]_n$ in which R-py are pyridine derivatives have been characterized. For 4-acpy (4-acetylpyridine) [59] or Minc (methylisonicotinate) [60], the compounds consist of manganese atoms with the two pyridinic ligands coordinated in *trans* and four end-to-end azido bridges, which link to the four neighboring manganese

atoms, giving a quadratic layer (Fig. 21). The two compounds show similar structural parameters in the bridging region: Mn–N–N bond angles of 129.0/151.6° and 128.3/149.7°, respectively. The Mn–N_3–Mn torsion angles are 98.1 and 94.6° for the 4-acpy and Minc compounds, respectively. As may be expected from the theoretical calculations, the coupling was antiferromagnetic for the two compounds, -3.83 cm^{-1} (4-acpy) and -2.24 cm^{-1} (Minc). Owing to canting phenomena, the $[Mn(4\text{-acpy})_2(N_3)_2]_n$ compound shows long range order below the $T_c = 28$ K and spontaneous magnetization and hysteresis loop measured at 2 K [61].

7.1.2. EE and EO bridges

With Ni^{II} and the 2,2′-dimethyl-propanediamine ligand (2,2′-mettn), a new two-dimensional system with ferro–antiferromagnetic alternation has been obtained: $[Ni(2,2\text{-mettn})(\mu\text{-}N_3)]_n$ [62,63]. In this complex each bridging azido ligand coordinates two Ni^{II} ions in an EO mode but, at the same time, this same azido ligand coordinates the neighboring Ni^{II} ion in an EE coordination mode (Fig. 22). This linkage is extended through a layer and the layers are linked by hydrogen and van der Waals forces. The main interest of this system lies in its magnetic properties: it shows a *canting* phenomenon at low temperature. The *canting* behavior can be defined as antiparallel spins canted with a small angle. The total result of these small vectors is not zero when the *canting* angle varies from zero. This *canting* gives the complex the characteristics of a molecular magnet (hysteresis loop, for example). It is, on the other hand, the molecular complex that shows this canting phenomenon at the highest temperature (close to 50 K).

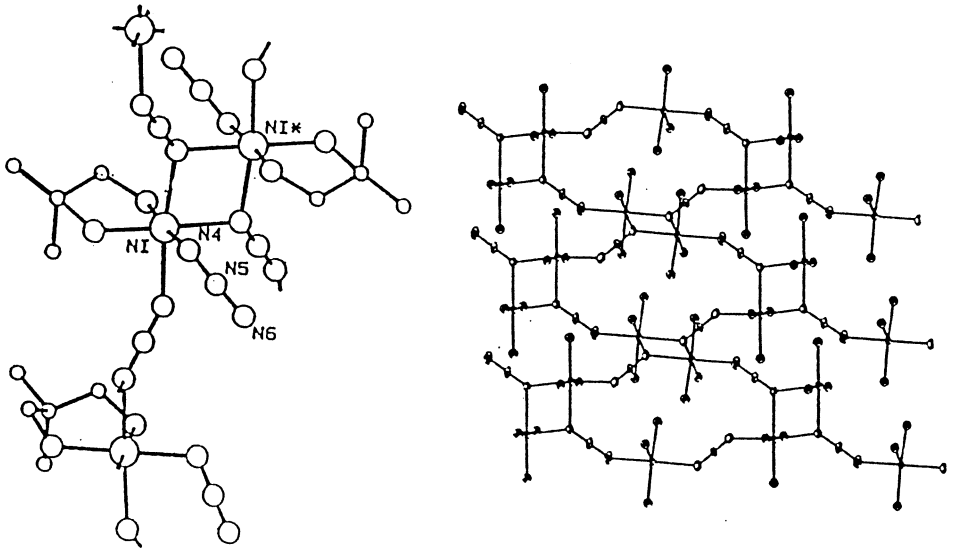

Fig. 22. Structure of the two-dimensional compound $[Ni(2,2\text{-mettn})(\mu\text{-}N_3)]_n$ (2,2-mettn = 2,2-dimethyl-propane-1,3-diamine).

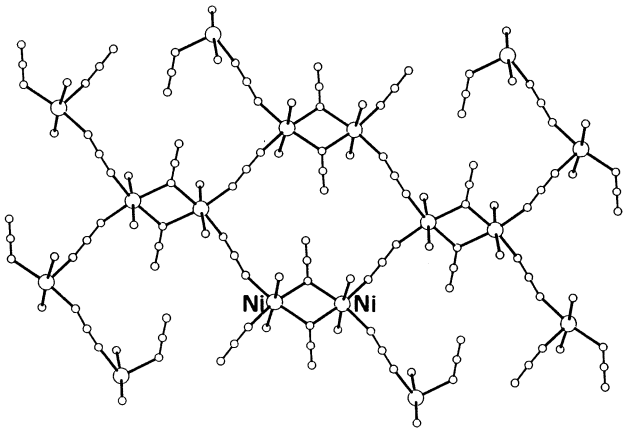

Fig. 23. General structure of the two-dimensional compounds $[Ni(amine)(N_3)_2]_n$ (amine = *N*-isopropylethylenediamine, *N*,*N*-diethylethylenediamine and *N*,*N*-diethyl-*N*′-methylethylenediamine).

For *N*-isopropylethylenediamine, *N*,*N*-diethylethylenediamine and *N*,*N*-diethyl-*N*′-methylethylenediamine three new two-dimensional complexes of general formula $[Ni(amine)(\mu\text{-}N_3)_2]_n$ have recently been reported [64]. The structural arrangement is the same in each case, consisting of dinuclear nickel units bridged by means of double EO azido bridges, linked to the four equivalent units by means of four single EE azido bridges (Fig. 23).

To describe the magnetic data a simplified pattern based on a sphere form of eight local $S = 1$ centers was designed using the full-diagonalization matrix method [65]. The two J values are ferromagnetic for the three complexes. Main structural and magnetic parameters are gathered in Table 8.

The same structure was found previously in four Mn^{II} compounds with the general formula $[Mn(R\text{-}py)_2(N_3)_2]_n$ in which R-py is Etnic (ethylisonicotinate) [66], 4-CNpy (4-cyanopyridine), 3-acpy (3-acetylpyridine) [61] and Enic (ethylnicotinate) [67]. Bridging bond parameters are similar, with the EO Mn–N–Mn bond angle

Table 8
Structural and magnetic parameters for 2-D Ni^{II} ferromagnetic compounds[a]

	Ni–N–N	Ni–N–Ni	τ	J	Reference
$[Ni(N\text{-ipen})(\mu\text{-}N_3)_2]_n$	125.9	99.3	116.8	27.3	64
	132.6			1.3	
$[Ni(N,N\text{-deen})(\mu\text{-}N_3)_2]_n$	132.5	100.9	112.8	30.2	64
	134.8			0.8	
$[Ni(N,N\text{-de-}N'\text{-men})(\mu\text{-}N_3)_2]_n$	137.5	100.5	110.4	26.1	64
	145.0			9.4	

[a] Ni–N–Ni angles (°); Ni–N–N angles (°); Ni–N_3–Ni τ angles (°); J in cm^{-1} (*N*-ipen = *N*-isopropylethylenediamine; *N*,*N*-deen = *N*,*N*-diethylethylenediamine; *N*,*N*-de-*N*′-men = *N*,*N*-diethyl-*N*′-methylethylenediamine).

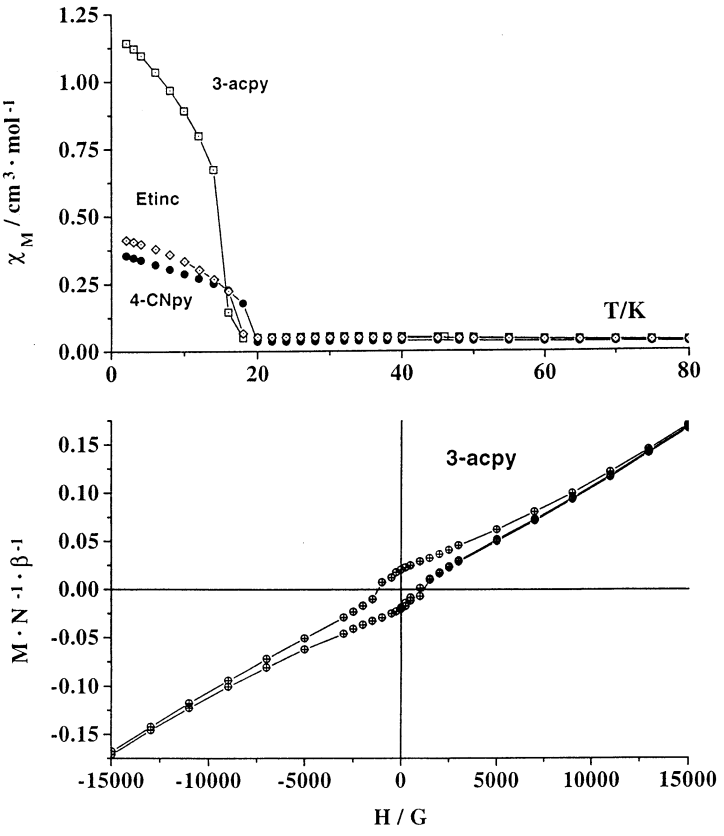

Fig. 24. Typical properties derived from the canting phenomenon in $[MnL_2(\mu\text{-}N_3)_2]_n$.

between 100.5 and 104.1° and Mn–N_3–Mn torsion angles (τ) comprised between 124.7 and 114.7°. J parameters were not calculated because the analytical expressions for alternating 2-D systems were not available, but as expected, the magnetic behavior corresponds to a ferro–antiferromagnetic system. Magnetic data for Enic compound were not reported, but for the other three compounds long range order was found at 16 K (Etnic and 3-acpy) and 28 K (4-CNpy). The typical properties derived from the canting phenomenon including hysteresis loop, broadening of the EPR signal when T is close to the T_c were characterized, [61] (Fig. 24).

7.2. Compounds with azide and a second bridging ligand

Alternating 2-D systems of manganese have been obtained following a similar strategy by using a second bridging group: the first of these with carboxylate bridges, with formula $[Mn(py2c)(N_3)(H_2O)]_n$, Hpy2c = pyridine 2-carboxylic acid [68], in which the oxygen atoms from the carboxylate group act as a bridge between two manganese atoms by means of one of the oxygen atoms, giving a dinuclear

entity Mn_2O_2 (Mn–O–Mn = 105.9°). Each unit is linked to four similar units by means of four end-to-end azido bridges with normal Mn–N–N bond angles of 139.5 and 127.4°. From the bond parameters in the bridging region and the coordination mode of the azido groups, antiferromagnetic behavior should be expected, but the magnetic data were not reported.

After a variety of experiments, substitution of the bipyridine ligand by that of the bipyrimidine (bipym) in the alternating ferro–antiferromagnetic 1-D compound $[Mn(bpy)(\mu_{1,1}\text{-}N_3)(\mu_{1,3}\text{-}N_3)]$ [55] led to the formation of the 2-D complex $[Mn_2(\mu_{1,1}\text{-}N_3)_4(\mu\text{-bipym})]_n$ [69]. The crystal structure of this compound shows chains of Mn^{II} ions connected by double 1,1-N_3 azido bridges. These chains are alternatively connected by bis-bidentate bipyrimidine ligands (Fig. 25). The whole structure can also be described as a honeycomb sheet, consisting of an infinite hexagonal array of Mn^{II} ions bridged by bis-bidentate bipyrimidine ligands and double end-on azido bridges. This 2-D polymer extends in the *xy* plane by the repetition of almost circular rings (Fig. 25).

The magnetic measurements for this 2-D indicates ferromagnetic interactions in the high temperature range, followed by antiferromagnetic interactions corresponding to the low temperature. Unfortunately, the lack of a theoretical model for this magnetic plane has precluded a detailed analysis of its magnetic behavior to date.

8. Three-dimensional systems

3-D compounds represent a challenge for researchers in the field of magnetic molecular systems. This is because of the need both to understand their magneto–structural correlations and to obtain 3-D antiferro- or ferromagnets with possible technical applications. 3-D systems with azido bridging group could be

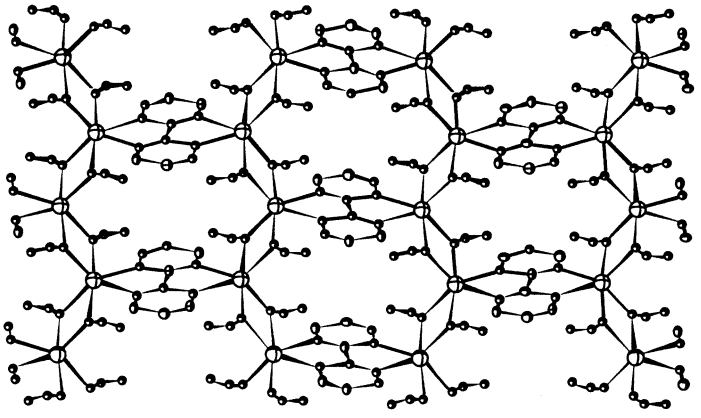

Fig. 25. Structure of the 'honeycomb' 2-D complex $[Mn(\mu_{1,1}\text{-}N_3)(\mu\text{-bipym})]_n$.

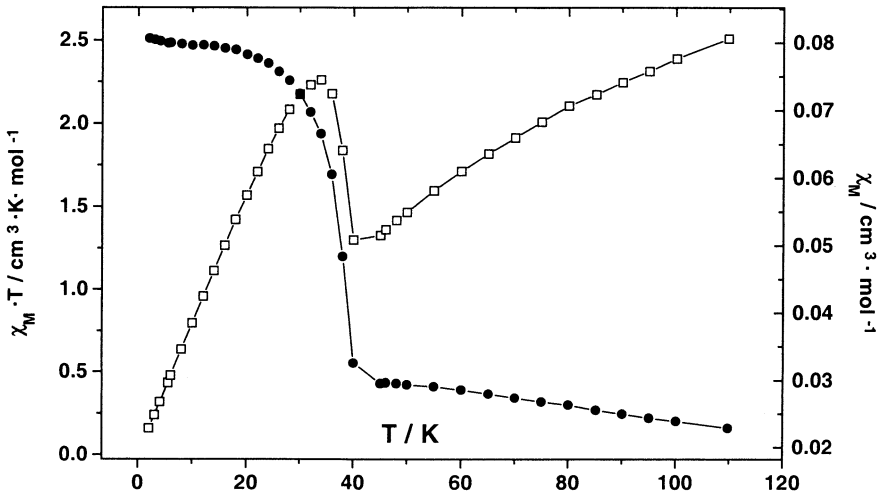

Fig. 26. Plot of $\chi_M T$ (●) and χ_M (○) of $[Mn(py)_2(\mu_{1,3}\text{-}N_3)_2]_n$ as a function of the temperature showing the high T_c of 40 K for the long range order.

obtained by either using metal:monodentate ligands in a 1:1 ratio, connecting 2-D compounds through *trans*-bidentate ligands or by preparation without the use of ancillary blocking ligands.

One 3-D compound, $[Mn(py)_2(\mu_{1,3}\text{-}N_3)_2]_n$ has been obtained using this last approach [70]. The compound shows a *trans* arrangement of the pyridine ligands and four EE bridges to the neighboring manganese atoms in a similar way to the 2-D compounds with R = 4-acpy or Minc. In these 2-D compounds the pyridine-like ligands are placed above and below the two-dimensional sheet, whereas in the 3-D arrangement the py ligands are placed along channels. Bond angles lie in the normal range, Mn–N–N = 134.1 and 145.4°, and magnetically show the expected antiferromagnetic coupling, with $J = -1.35$ cm^{-1} (Fig. 26). The high T_c of 40 K is noticeable for the long range order with the presence of a canting phenomenon [61].

A second 3-D compound with only azide bridges was $[N(CH_3)_4]_n[Mn(\mu_{1,3}\text{-}N_3)_3]_n$ [71]. The proportion of three azido ligands per divalent ion was achieved by using an appropriate cation. The crystal structure of the compound is shown in Fig. 27. This structure may be described as a distorted perovskite where the Mn^{II} is shifted from the origin of the unit cell by ca. 0.25 Å along the *b*-axis. The azido groups act as end-to-end bridging ligands between metals to form the 3-D network. Each manganese ion shows a slightly distorted octahedral coordination sphere. The $[N(CH_3)_4]^+$ cations are located within the holes formed by the Mn^{II}-azido sublattice (Fig. 27). The $\mu_{1,3}$-N_3 bridges form two asymmetric angles with the metal: Mn–N–N around 165° and N–N–Mn′ around 135°.

The magnetic measurements for this complex clearly indicate the existence of AF interactions (Fig. 27). The magnetic behavior can be explained assuming a

regular 3-D network as indicated by the crystal structure. The best least-square fit of the experimental data to the expression of the magnetic susceptibility for a simple cubic Heisenberg antiferromagnetic system [72] is obtained with the parameters $J = -1.21$ cm^{-1} and $g = 2.01$.

A new example of 3-D Mn^{II} azido compound is a polymorph of the 2-D $[Mn_2(\mu_{1,1}\text{-}N_3)_4(\mu\text{-bipym})]_n$ system [69], with the formula $[Mn_2N_3(\mu_{1,1}\text{-}N_3)(\mu_{1,3}\text{-}N_3)(\mu\text{-bipym})]_n$, [69b]. The crystal structure consists of chains of manganese atoms alternately bridged by bipym and two end-on azido groups (Fig. 28). The chains are connected by means of end-to-end azido groups in vicinal positions, which ensures linkages in two different directions. Its magnetic properties are in

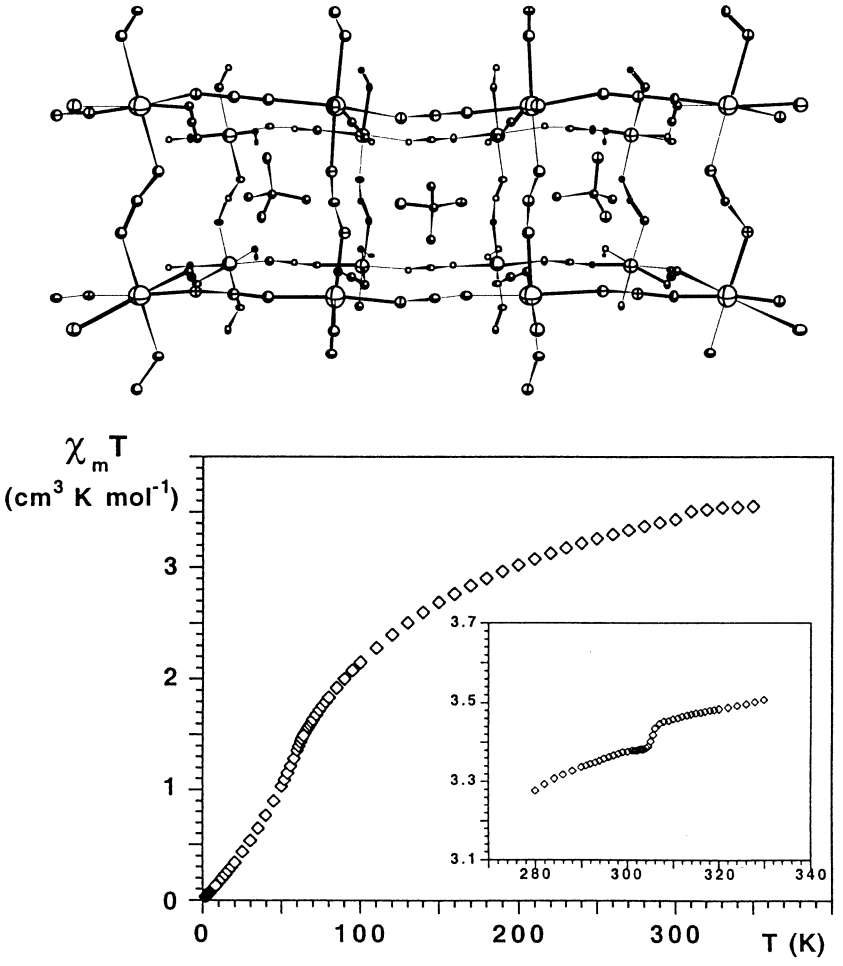

Fig. 27. Structure of the three-dimensional compound $[N(CH_3)_4]_n[Mn(\mu_{1,3}\text{-}N_3)_3]_n$ (top) and $\chi_M T$ (□) of this compound as a function of the temperature.

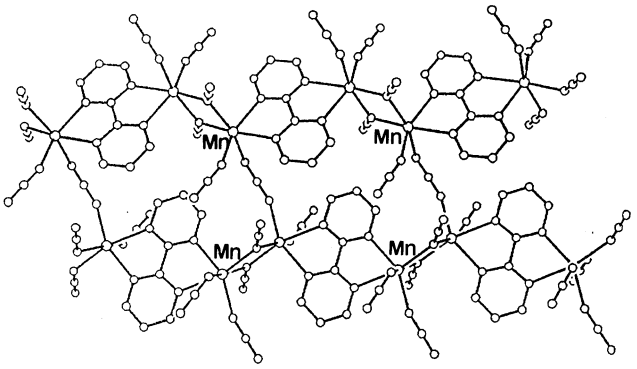

Fig. 28. Structure of the three-dimensional compound $[Mn_2N_3(\mu_{1,1}\text{-}N_3)(\mu_{1,3}\text{-}N_3)(\mu\text{-bipym})]_n$.

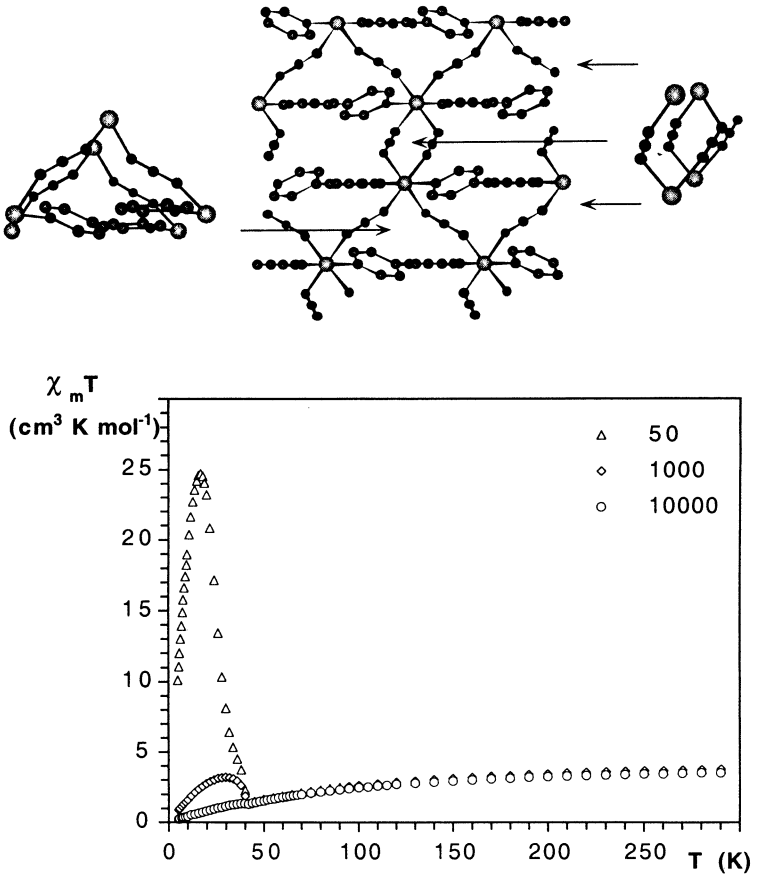

Fig. 29. Structure of the three-dimensional compound $[Mn(\mu-4,4'\text{-bpy})(\mu_{1,3}N_3)_2]_n$ complex showing the helical chains of Mn^{II} ions of two different types (top) and $\chi_M T$ of this compound as a function of the temperature at different magnetic fields.

accord with predominant antiferromagnetic interactions, which are propagated by the bipym and the end-to-end azido bridges and which are larger than the ferromagnetic interactions corresponding to the end-on azido bridges.

Another interesting example of 3-D Mn^{II}-azido systems is the [Mn(μ-4-4′-bpy)($\mu_{1,3}$-N_3)$_2$] complex [73]. The crystal structure (Fig. 29) shows helical chains of Mn^{II} ions of two different types. The chains of the first type are connected by single EE azido bridges (–Mn–N_3–Mn–N_3–), while the second type exhibit two consecutive EE azido bridges, followed by 4,4′-bipyridine bridges (–Mn–N_3–Mn–N_3–Mn–4,4′-bpy–). The whole structure has the form of a complex 3-D network as a result of the propagation of these different helicals. The Mn^{II} ion exhibits a slightly distorted octahedral environment formed by six nitrogen atoms, four from the azido and two from the 4,4′-bpy, respectively. The Mn–N distances range from 2.185(6) to 2.301(4) Å (bpy). The EE azido bridges form two asymmetric angles with the metal, with values of 153.0(5) and 121.9(4)°.

The magnetic behavior of this complex is characteristic of a system with antiferromagnetic interactions in the high temperature region, up to 50 K, where a magnetic transition to a ferromagnetic state occurs. The temperature dependence of the molar magnetization was investigated within a magnetic field of 50 Gauss. The 'field-cooled' magnetization showed an abrupt break at $T_c = 45$ K which is characteristic of a magnetically ordered state existing below 45 K [74].

The field dependence behavior of the magnetization at 5 K can be assigned to an antiferromagnetic system with a weak ferromagnetic component. At magnetic fields lower than 2500 Gauss, magnetic hysteresis is observed. This kind of behavior is probably due to a canting phenomenon.

Acknowledgements

The authors thank the Spanish government (Grant PB96/0163) and the Basque government (Grant PI96/39) for the financial support.

References

[1] R.D. Willet, D. Gatteschi, O. Kahn (Eds.), Magneto–Structural Correlations in Exchange Coupled Systems, NATO ASI Series, Reidel, Dordrecht, 1985.
[2] O. Kahn, Molecular Magnetism, VCH Publishers, Weinheim, 1993.
[3] M.M. Turnbull, T. Sugimoto, L.K. Thompson (Eds.), Molecular-Based Magnetic Materials: Theory, Techniques and Applications. ACS Symposium Series, n.644, ACS, Washington, 1996.
[4] A. Caneschi, D. Gatteschi, L. Pardi, R. Sessoli, Clusters, Chains and Layered Molecules: the Chemist's Way to Magnetic Materials, in: A.F. Williams (Ed.), Perspectives in Coordination Chemistry, VCH, Weinheim, 1992.
[5] E. Coronado, P. Delhaes, D. Gatteschi, J.S. Miller (Eds.), Molecular Magnetism: from Molecular Assemblies to Devices, NATO ASI Series, Vol.321, Kluwer, Dordrecht, 1995.
[6] D.W. Bruce, D. O'Hare (Eds.), Inorganic Materials, Wiley, 1992.
[7] P. Delhaes, M. Drillon (Eds.), Organic and Inorganic Low-Dimensional Materials, NATO ASI Series, vol. 168, Plenum Press, NY, 1987.

[8] D. Gatteschi, O. Kahn, J.S. Miller, F. Palacio (Eds.), Magnetic Molecular Materials. NATO ASI Series, Vol.198. Kluwer, Dordrecht, 1993.
[9] C.J. O'Connor (Ed.), Research Frontiers in Magnetochemistry. World Scientific, Singapore, 1993.
[10] J. Commarmond, P. Plumeré, J.M. Lehn, Y. Agnus, R. Louis, R. Weiss, O. Kahn, I. Morgensten-Badarau, J. Am. Chem. Soc. 104 (1982) 6330.
[11] (a) M.F. Charlot, O. Kahn, M. Chaillet, C. Larrieu, J. Am. Chem. Soc. 108 (1986) 2574. (b) M.A. Aebersold, B. Gillon, O. Platevin, L. Pardi, O. Kahn, P. Bergerat, I. von Seggern, F. Tuczek, L. Ohrstrom, A. Grand, E. Levièvre-Berna, J. Am. Chem. Soc. 120 (1998) 5238.
[12] A. Bencini, C.A. Ghilardo, S. Midollini, A. Orlandini, Inorg. Chem. 28 (1989) 1958.
[13] O. Kahn, T. Mallah, J. Gouteron, S. Jeannin, Y. Jeannin, J. Chem. Soc. Dalton Trans. (1989) 1117.
[14] (a) O. Castell, R. Caballol, V.M. García, K. Handrick, Inorg. Chem. 35 (1996) 1609. (b) E. Ruiz, J. Cano, S. Alvarez, P. Alemany, J. Am. Chem. Soc. 120 (1998) 11122
[15] (a) M.I. Arriortua, R. Cortés, L. Lezama, T. Rojo, X. Solans, M. Font-Bardía, Inorg. Chim. Acta 174 (1990) 263. (b) T. Rojo, L. Lezama, R. Cortés, J.L. Mesa, M.I. Arriortua, J. Magn. Mat. 83 (1990) 519. (c) R. Cortés, L. Lezama, T. Rojo, M. Karmele Urtiaga, M. Isabel Arriortua, IEEE Trans. on Magn. 30 (1994) 4728
[16] R. Cortés, K. Urtiaga, L. Lezama, J.L. Pizarro, A. Goñi, M.I. Arriortua, T. Rojo, Inorg. Chem. 33 (1994) 4009.
[17] A. Escuer, R. Vicente, J. Ribas, M.S. El Fallah, X. Solans, M. Font-Bardía, Inorg. Chem. 32 (1993) 3727.
[18] A. Escuer, R. Vicente, J. Ribas, M.S. El Fallah, X. Solans, M. Font-Bardía, Adv. Mater. Res. 1 (1994) 581.
[19] A. Escuer, R. Vicente, M.S. El Fallah, X. Solans, M. Font-Bardía, J. Chem. Soc. Dalton Trans. (1996) 1013.
[20] A. Escuer, R. Vicente, X. Solans, M. Font-Bardía, Inorg. Chem. 33 (1994) 6007.
[21] J. Ribas, M. Monfort, C. Diaz, C. Bastos, X. Solans, Inorg. Chem. 32 (1993) 3557.
[22] J. Ribas, M. Monfort, C. Diaz, A. Escuer, R. Vicente, M.S. El Fallah, X. Solans, M. Font-Bardía, Adv. Mater. Res. 1 (1994) 573.
[23] (a) R. Vicente, A. Escuer, J. Ribas, X. Solans, Inorg. Chem. 31 (1992) 1726. (b) R. Vicente, A. Escuer, Polyhedron 14 (1995) 2133.
[24] P. Chaudhuri, T. Weyhermüller, E. Bill, K. Wieghardt, Inorg. Chim. Acta 252 (1996) 195.
[25] D.M. Duggan, D.N. Hendrickson, Inorg. Chem. 13 (1974) 2929.
[26] C.G. Pierpont, D.N. Hendrickson, D.M. Duggan, F. Wagner, E.K. Barefield, Inorg. Chem. 14 (1975) 604.
[27] F. Wagner, M.T. Mocella, M.J.J. D'Aniello, A.H.J. Wang, E.K. Barefield, J. Am. Chem. Soc. 96 (1974) 2625.
[28] G.A. McLachlan, G.D. Fallon, R.L. Martin, B. Moubaraki, K.S. Murray, L. Spiccia, Inorg. Chem. 33 (1994) 4663.
[29] (a) L. Fabrizzi, P. Pallavicini, L. Parodi, A. Perotti, N. Sardone, A. Taglietti, Inorg. Chim. Acta 244 (1996) 7. (b) A. Escuer, C.J. Harding, Y. Dussart, J. Nelson, V. McKee, R. Vicente, J. Chem. Soc. Dalton Trans. (1999) 223.
[30] H. Weller, L. Siegfried, M. Neuburger, M. Zenhder, T.A. Kaden, Helvetica Chim. Acta 80 (1997) 2315.
[31] P.J. Hay, J.C. Thibeault, R. Hoffmann, J. Am. Chem. Soc. 97 (1975) 4884.
[32] R. Cortés, K. Urtiaga, L. Lezama, M.L. Rodríguez, M.I. Arriortua, T. Rojo, Inorg. Chem., submitted for publication
[33] P. Chaudhuri, M. Guttmann, D. Ventur, K. Wieghardt, B. Nuber, J. Weiss, J. Chem. Soc. Chem. Commun. (1985) 1618.
[34] A.P. Ginsberg, R.L. Martin, R.W. Brookes, R.C. Sherwood, Inorg. Chem. 11 (1972) 2884.
[35] A. Escuer, R. Vicente, J. Ribas, X. Solans, Inorg. Chem. 34 (1995) 1793.
[36] M.A.S. Goher, F.A. Mautner, A. Popitsch, Polyhedron 12 (1993) 2557.
[37] R. Cortés, J.L. Pizarro, L. Lezama, M.I. Arriortua, T. Rojo, Inorg. Chem. 33 (1994) 2697.
[38] P.D. Beer, M.G.B. Drew, P.B. Leeson, K. Lyssenko, M.I. Ogden, J. Chem. Soc. Chem. Commun. (1995) 929.

[39] A. Escuer, I. Castro, F.A. Mautner, M.S. El Fallah, R. Vicente, Inorg. Chem. 36 (1997) 4633.
[40] J. Ribas, M. Monfort, R. Costa, X. Solans, Inorg. Chem. 32 (1993) 695.
[41] M.A. Halcrow, J.C. Huffman, G. Christou, Angew. Chem. Int. Ed. Engl. 34 (1995) 889.
[42] M.A. Halcrow, J.-S. Sun, J.C. Huffman, G. Christou, Inorg. Chem. 34 (1995) 4167.
[43] K. Urtiaga, Z.E. Serna, G. Barandika, L. Lezama, M.I. Arriortua, R. Cortés, Proceedings of the XXXIII ICCC, p. 421.
[44] S. Brooker, V. McKee, J. Chem. Soc. Chem. Commun. (1989) 619.
[45] A. Escuer, R. Vicente, J. Ribas, M.S. El Fallah, X. Solans, M. Font-Bardía, Inorg. Chem. 33 (1994) 1842.
[46] C. Mealli, D.M. Proserpio, J. Chem. Educ. 67 (1990) 3399.
[47] (a) L.K. Chou, D.R. Talham, W.W. Kim, P.J.C. Signore and M.W. Meisel, Physica B 194 (1994) 313. (b) T. Takeuchi, H. Hori, M. Date, T. Yosida, K. Katsumata, J.P. Renard, V. Gadet, M. Verdaguer, J. Magn. Magn. Mat. 104 (1992) 813. (c) T. Takeuchi, T. Yosida, K. Inoue, M. Yamashita, T. Kumada, K. Kindo, S. Merah, M. Verdaguer, J.P. Renard, J. Magn. Magn. Mat. 140 (1995) 1633.
[48] A. Escuer, R. Vicente, M.A.S. Goher, F.A. Mautner, Inorg. Chem. 37 (1998) 782.
[49] J. Ribas, M. Monfort, C. Diaz, C. Bastos, X. Solans, Inorg. Chem. 33 (1994) 484.
[50] T. de Neef, PhD Thesis, Eindhoven, 1975.
[51] A. Escuer, R. Vicente, F.A. Mautner, M.A.S. Goher, Proceedings of the XXXIII ICCC, p.356.
[52] J.J. Borrás-Almenar, E. Coronado, J. Curély, R. Georges, Inorg. Chem. 34 (1995) 2699.
[53] (a) M. Hagiwara, Y. Narumi, K. Kindo, M. Kohno, H. Nakano, R, Sato, M. Takahashi, Phys. Rev. Lett. 80 (1998) 1312. (b) M. Kohno, M. Takahashi, M. Hagiwara, Phys. Rev. B, 57 (1998) 1046.
[54] (a) J. Ribas, M. Monfort, I. Resino, X. Solans, P. Rabu, F. Maingot, M. Drillon, Angew. Chem. Int. Ed. Engl. 35 (1996) 2520. (b) F. Esposito, G. Kamieniarz, Phys. Rev. B 57 (1998) 7431.
[55] (a) R. Cortés, L. Lezama, J.L. Pizarro, M.I. Arriortua, X. Solans, T. Rojo, Angew. Chem. Int. Ed. Eng. 33 (1994) 2488. (b) R. Cortés, M. Drillon, X. Solans, L. Lezama, T. Rojo, Inorg. Chem. 36 (1997) 677.
[56] A. Escuer, R. Vicente, M.S. El Fallah, S.B. Kumar, F.A. Mautner, D. Gatteschi, J. Chem. Soc. Dalton Trans. (1998) 3905.
[57] J. Ribas, M. Monfort, B. Kumar-Gosh, X. Solans, Angew. Chem. Int. Ed. Engl. 33 (1994) 2087.
[58] H.E. Maier, H. Krischner, H. Paulus, Zeitschrift für Kristallographie 157 (1981) 277.
[59] A. Escuer, R. Vicente, M.A.S. Goher, F.A. Mautner, Inorg. Chem. 34 (1995) 5707.
[60] A. Escuer, R. Vicente, M.A.S. Goher, F.A. Mautner, J. Chem. Soc. Dalton Trans. (1997) 4431.
[61] A. Escuer, R. Vicente, M.A.S. Goher, F.A. Mautner, Inorg. Chem. 36 (1997) 3440.
[62] M. Monfort, J. Ribas, X. Solans, J. Chem. Soc. Chem. Commun. (1993) 350.
[63] J. Ribas, M. Monfort, X. Solans, M. Drillon, Inorg. Chem. 33 (1994) 742.
[64] M. Monfort, J. Ribas, I. Resino, M.S. El Fallah, H. Stoeckly-Evans, Proceedings of the XXXIII ICCC, p.386.
[65] CLUMAG Program, D. Gatteschi, L. Pardi, Gazz. Chim. Ital 123 (1993) 231.
[66] A. Escuer, R. Vicente, M.A.S. Goher, F.A. Mautner, Inorg. Chem. 35 (1996) 6386.
[67] M.A.S. Goher, N.A. Al-Salem, F.A. Mautner, J. Coord. Chem. 44 (1998) 119.
[68] M.A.S. Goher, M.A.M. Abu-Youssef, F.A. Mautner, A. Popitsch, Polyhedron 11 (1992) 2137.
[69] (a) G. De Munno, M. Julve, G. Viau, F. Lloret, J. Faus, D. Viterbo, Angew. Chem. Int. Ed. Engl. 35 (1996) 1807. (b) R. Cortés, L. Lezama, J.L. Pizarro, M.I. Arriortua, T. Rojo, Angew. Chem. Int. Ed. Engl. 35 (1996) 1810. (c) R. Cortés, M.K. Urtiaga, L. Lezama, J.L. Pizarro, M.I. Arriortua, T. Rojo, Inorg. Chem. 36 (1997) 5016.
[70] M.A.S. Goher, F.A. Mautner, Croat. Chim. Acta 63 (1990) 559.
[71] F.A. Mautner, R. Cortés, L. Lezama, T. Rojo, Angew. Chem. Int. Ed. Engl. 35 (1996) 78.
[72] G.S. Rushbrook, P.J. Wood, Mol. Phys. 1 (1958) 257.
[73] (a) R. Cortés, S. Martín, L. Lezama, J.L. Pizarro, M.I. Arriortua, T. Rojo, Inorg. Chem., submitted for publication. (b) H.Y. Shen, D.Z. Liao, Z.H. Jiang, S.P. Yan, B.W. Sun, G.L. Wang, X.K. Yao, H.G. Wang, Chem. Lett. (1998) 469.

[74] R. Cortés, S. Martín, L. Lezama, G. Barandika, T. Rojo, J.L. Pizarro, Proceedings of the XXXIII ICCC, p. 352.
[75] J. Ribas, M. Monfort, B. Kumar-Gosh, R. Cortés, X. Solans, M. Font-Bardía, Inorg. Chem. 35 (1996) 864.
[76] A. Escuer, R. Vicente, M.S. El Fallah, X. Solans, M. Font-Bardía, Inorg. Chim. Acta 278 (1998) 43.
[77] R. Cortés, J.I.R. Larramendi, L. Lezama, T. Rojo, K. Urtiaga, M.I. Arriortua, J. Chem. Soc. Dalton Trans. (1992) 2723.
[78] R. Vicente, A. Escuer, J. Ribas, M.S. El Fallah, X. Solans, M. Font-Bardía, Inorg. Chem. 32 (1993) 1920.
[79] A. Escuer, R. Vicente, J. Ribas, J. Magn. Magn. Mater. 110 (1992) 181.
[80] A. Escuer, R. Vicente, M.S. El Fallah, X. Solans, M. Font-Bardía, Inorg. Chim. Acta 247 (1996) 85.
[81] R. Cortés, L. Lezama, J.I.R. Larramendi, M. Insausti, J.V. Folgado, G. Madariaga, T. Rojo, J. Chem. Soc. Dalton Trans. (1994) 2573.
[82] X. Solans, C.Diaz, M.Monfort, J.Ribas, XV International Crystallographic Meeting. Burdeos, 1990
[83] M. Monfort, J. Ribas, X. Solans, M. Font-Bardía, Inorg. Chem. 35 (1996) 7633.
[84] C. Bastos, C. Diaz, M. Monfort, J. Ribas, X. Solans, Abstracts 29th ICCC, Lausanne, 1992, p. 644.
[85] A. Escuer, R. Vicente, J. Ribas, M.S. El Fallah, X. Solans, Inorg. Chem. 32 (1993) 1033.
[86] R. Vicente, A. Escuer, J. Ribas, M.S. El Fallah, X. Solans, M. Font-Bardía, Inorg. Chem. 34 (1995) 1278.
[87] A. Escuer, R. Vicente, M.S. El Fallah, J. Ribas, X. Solans, M. Font-Bardía, J. Chem. Soc. Dalton Trans. (1993) 2975.
[88] J. Ribas, M. Monfort, C. Diaz, C. Bastos, C. Mer, X. Solans, Inorg. Chem. 34 (1995) 4986.
[89] (a) G. Viau, M.G. Lombardi, G. De Munno, M. Julve, F. Lloret, J. Faus, A. Caneschi, J.M. Clemente-Juan, J. Chem. Soc. Chem. Commun. (1997) 1195. (b) J.J. Borrás-Almenar, J.M. Clemente-Juan, E. Coronado, F. Lloret, Chem. Phys. Lett. 275 (1997) 79
[90] J. Ribas, M. Monfort, B. Kumar-Gosh, X. Solans, M. Font-Bardía, J. Chem. Soc. Chem. Commun. (1995) 2375.